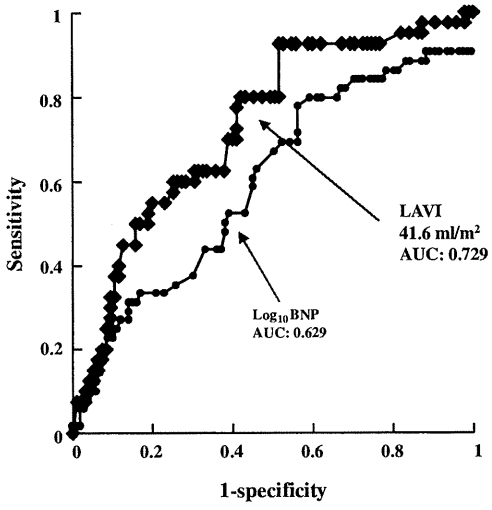

Fig. 1. Receiver operating characteristic (ROC) curve analyses of left atrial volume index (LAVI) and $\log_{10}$ B-type natriuretic peptide (BNP) for predicting cardiac events. The area under the ROC curve (AUC) for LAVI was 0.729. LAVI >41.6 mL/m^2 had a sensitivity of 80% and a specificity of 58%. The AUC for LAVI was greater than that for $\log_{10}$ BNP.

medication use between patients with and without cardiac events.

Risk Stratification by LAVI and Clinical Outcome

LAVI increased with worsening NYHA functional class. The ROC curve for LAVI as a predictor of cardiac events is shown in Figure 1. The AUC for LAVI was 0.729. LAVI >41.6 mL/m^2 had a sensitivity of 80% and a specificity of 58% for cardiac events. In addition, the AUC for LAVI as a predictor of cardiac events was 0.758 in patients with sinus rhythm, which was larger than that in all patients, including patients with AF.

The ROC curves obtained for LAVI and $\log_{10}$ BNP at discharge were compared (Fig. 1). The sensitivity and specificity of $\log_{10}$ BNP for detecting cardiac events were 67% and 54%, respectively. The AUC for LAVI (0.729) was greater than that for $\log_{10}$ BNP (0.629), suggesting that LAVI was superior to $\log_{10}$ BNP for predicting adverse outcomes.

Table 2. Results of Univariate Cox Proportional Hazard Analysis

Variable	Hazard Ratio	95% CI	*P* Value
Age (per 1 y increase)	1.006	0.981–1.032	.6564
NYHA functional class III-IV (at admission)	2.702	1.063–6.897	.0368
AF	1.325	0.719–2.443	.3671
LVDd (per 1 SD increase)	0.992	0.968–1.016	.5063
LVEF (per 1 SD increase)	0.985	0.965–1.004	.1273
MR moderate	2.024	1.037–3.953	.0385
E/E′ (per 1 SD increase)	1.316	1.028–1.670	.0281
LAVI (per 1 SD increase)	1.461	1.154–1.803	.0010
Creatinine (per 1 SD increase)	1.251	1.025–1.526	.0276
$\log_{10}$ BNP at admission (per 1 SD increase)	1.512	0.771–2.967	.2290
$\log_{10}$ BNP at discharge (per 1 SD increase)	2.957	1.487–5.883	.0020

CI, confidence interval; MR, mitral regurgitation; other abbreviations as in Table 1.

Table 3. Results of Multivariate Cox Proportional Hazard Analysis

Variable	Hazard Ratio	95% CI	*P* Value
Age (per 1 y increase)	0.987	0.959–1.015	.3563
NYHA functional class III-IV (at admission)	3.205	1.103–9.346	.0324
AF	1.046	0.467–2.343	.9133
LVDd (per 1 SD increase)	0.547	0.266–1.113	.0966
MR moderate	0.466	0.217–1.002	.0605
E/E′ (per 1 SD increase)	1.175	0.878–1.574	.2827
LAVI (per 1 SD increase)	1.427	1.024–1.934	.0317
Creatinine (per 1 SD increase)	1.158	0.923–1.453	.2035
$\log_{10}$ BNP at discharge (per 1 SD increase)	1.471	1.019–2.123	.0395

Abbreviations as in Tables 1 and 2.

Simple linear regression analysis showed that LAVI was correlated with E/E′ (r = 0.284; P = .0006).

The univariate Cox proportional hazard analysis revealed that LAVI was a significant prognostic factor for cardiac events (Table 2). $\log_{10}$ BNP at discharge, prevalence of NYHA functional class III-IV at admission, moderate MR, an increase in E/E′ of 1 SD, and serum creatinine levels were also related to cardiac events. In the multivariate Cox proportional hazard analysis, LAVI was an independent predictor of cardiac events after adjusting for age, NYHA functional class, AF, LVDd, and moderate MR (Table 3).

All patients were stratified into 3 groups according to tertiles for LAVI: <35.4 mL/m^2 (n = 49), 35.4–53.3 mL/m^2 (n = 49); and >53.3 mL/m^2 (n = 48). Kaplan-Meier analysis showed that there was a stepwise increase in risk of cardiac events with each increment of LAVI category, and LAVI >53.3 mL/m^2 was associated with the highest risk of cardiac events (log-rank test: P < .01; Fig. 2). As shown in Figure. 3, the relative risk of cardiac events was 4.9 times greater in the highest tertile compared with the lowest tertile.

Changes in LAVI Between Admission and Discharge

In 36 patients, LAVI was measured at both admission and discharge (Fig. 4). LAVI was greater at admission and tended to decrease at discharge after 22 ± 17 days in patients without cardiac events (51 ± 4 vs 44 ± 2 mL/m^2; P = .081). However, LAVI was high at both admission and discharge in patients with cardiac events (58 ± 7 vs 56 ± 4 mL/m^2; P = .4255).

Discussion

The present study demonstrated that LAVI was an independent predictor of adverse cardiac events in patients with HF.

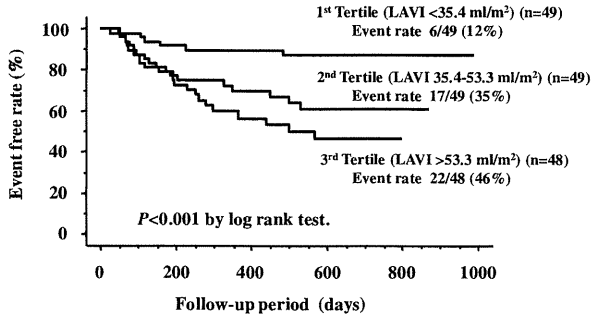

Fig. 2. Kaplan-Meier analysis showed that there was a stepwise increase in risk of cardiac events with each increment of left atrial volume index (LAVI) category, and LAVI >53.3 mL/m^2 was associated with the highest risk of cardiac events (log-rank test: $P < .01$).

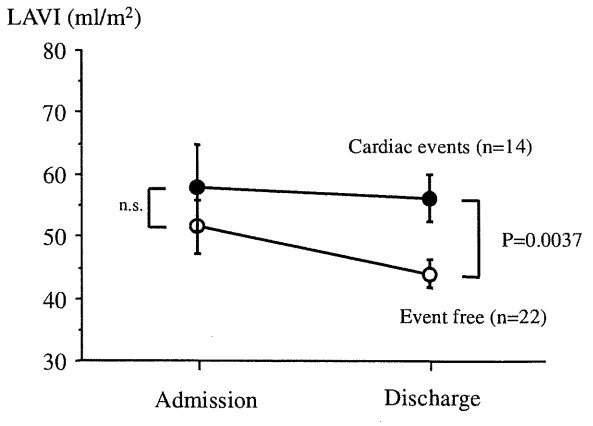

Fig. 4. Changes in left atrial volume index (LAVI) between admission and discharge. Results are expressed as mean ± SE.

Abnormal LV relaxation and decreased LV compliance may occur as a consequence of altered actin-myosin interactions and increased collagen deposition or cross-linking, with changes in cardiac viscoelastic properties.[18] Because the LA is directly exposed to LV filling pressure during the diastolic phase, a persistent increase in LA filling pressure leads to dilatation of the chamber and stretching of the atrial myocardium.[6,8] Therefore, LA volume may be a marker of the burden of LV diastolic dysfunction, which increases LA filling pressure[8] and LV end-diastolic pressure (LVEDP).[19] It is well known that LV systolic dysfunction is an important prognostic factor in HF. However, the incidence of HF with preserved ejection fraction has increased and now comprises nearly 50% of patients with HF,[19–22] suggesting that LV diastolic dysfunction may play an important role in the onset of HF. Tsang et al[23] reported that LAVI indicated the severity of diastolic dysfunction and provided an index of the burden of cardiovascular risk in patients without a history of AF or valvular heart disease. However, the prognostic value of LAVI in patients with HF has not been fully determined.

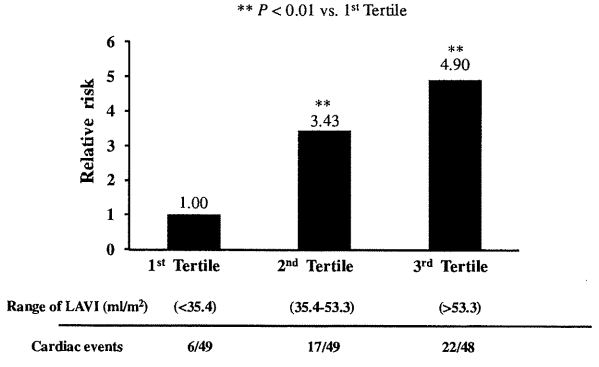

Fig. 3. Relative risk of cardiac events by tertiles of left atrial volume index (LAVI). The relative risk of cardiac events was greatest for patients in the third tertile of LAVI (**$P < .01$ versus first tertile).

LAVI was greater in patients with cardiac events than in those without cardiac events (Table 1). E/E′, which is a well known marker of LV diastolic dysfunction,[24] was also greater in patients with cardiac events. These results suggest that LAVI reflects increasing LVEDP and LA pressure caused by LV diastolic dysfunction. However, simple linear regression analysis showed a weak correlation ($r = 0.284$) between LAVI and E/E′, suggesting that these 2 parameters may have different prognostic significance. Furthermore, as shown in Table 3, LAVI was superior to E/E′ as a predictor of prognosis.

Whereas markers of LV diastolic dysfunction predicted a poor prognosis, LVEF was not a significant prognostic factor in the present study (Table 2). This may be attributed to the fact that in 51% of the enrolled patients LVEF was preserved (>45%). LAVI has been reported to be a powerful predictor of mortality and has remained an independent predictor after adjustment for clinical factors and LV systolic function in patients with acute myocardial infarction.[9] It was suggested that LA volume is less influenced by acute changes and reflects subacute or chronic function, whereas Doppler variables are affected by multiple factors and change rapidly. In the present study, patients with reduced LVEF (<45%) and a high LAVI (>41.6 mL/m^2) had a greater incidence of cardiac events (15/43 patients) compared with patients with reduced LVEF but a normal LAVI (5/28 patients). This result suggested that increased LAVI is a powerful predictor of cardiac events in patients with HF, and provides additional prognostic information to that provided by conventional parameters of LV function.

Plasma BNP levels at discharge are reportedly a better reflection of prognosis compared with levels measured at admission.[25] This is consistent with the results presented here (Table 2). Plasma BNP levels at discharge were significantly higher in patients with cardiac events than in those without cardiac events. Elevated plasma BNP levels at discharge may reflect the chronic increase in LA pressure, which causes dilatation of the LA chamber and stretching of the atrial myocardium. In 36 patients, LAVI was

measured at both admission and discharge, and the results suggested that a persistent increase in LAVI may be associated with adverse outcomes (Fig. 4).

Some earlier reports have suggested a relationship between LAVI and prognosis in patients with HF. Popescu et al[26] reported that LAVI was a better prognostic predictor than plasma BNP levels in 46 elderly patients with HF. Although that study population was small, the results are consistent with those from the present study. Lim et al[27] also reported that LAVI was an independent predictor of mortality in patients with suspected HF who were referred from the community. The LAVI cutoff value in that study was quite different from the present study and that of Popescu et al, probably because the study population was different.

Several earlier studies demonstrated that advanced diastolic dysfunction, characterized by an increased E/A ratio and shortening of the E-deceleration time, was strongly associated with increased mortality.[28–30] However, E/A ratio cannot be calculated in patients with AF, whose numbers continue to increase because of the aging population. In the present study, 36% of patients had AF; however, LAVI remained an independent predictor of cardiac events after adjustment for the prevalence of AF and moderate MR (Table 3). The multivariate Cox proportional hazard analysis and the ROC curve analysis revealed that LAVI was a more powerful prognostic predictor than plasma BNP level at discharge.

The present study has several limitations. First, the number of subjects studied was relatively small. Second, because echocardiography was not performed during follow-up, it was not possible to determine whether the long-term prognosis was affected by improvement in the LAVI.

In conclusion, LAVI is an independent prognostic factor for cardiac events and may be useful for risk stratification in patients with HF.

Disclosures

None.

References

1. Funk M, Krumholz HM. Epidemiologic and economic impact of advanced heart failure. J Cardiovasc Nurs 1996;10:1–10.
2. CONSENSUS Trial Study Group. Effects of enalapril on mortality in severe congestive heart failure. Results of the Cooperative North Scandinavian Enalapril Survival Study (CONSENSUS). N Engl J Med 1987;316:1429–35.
3. SOLVD Investigators. Effect of enalapril on survival in patients with reduced left ventricular ejection fractions and congestive heart failure. N Engl J Med 1991;325:293–302.
4. Vasan RS, Levy D. Defining diastolic heart failure: a call for standardized diagnostic criteria. Circulation 2000;101:2118–21.
5. Zile MR, Gaasch WH, Carroll JD, Feldman MD, Aurigemma GP, Schaer GL, et al. Heart failure with a normal ejection fraction: is measurement of diastolic function necessary to make the diagnosis of diastolic heart failure? Circulation 2001;104:779–82.
6. Appleton CP, Galloway JM, Gonzalez MS, Gaballa M, Basnight MA. Estimation of left ventricular filling pressures using two-dimensional and Doppler echocardiography in adult patients with cardiac disease. Additional value of analyzing left atrial size, left atrial ejection fraction and the difference in duration of pulmonary venous and mitral flow velocity at atrial contraction. J Am Coll Cardiol 1993;22:1972–82.
7. Basnight MA, Gonzalez MS. Kershenovich SC, Appleton CP. Pulmonary venous flow velocity: relation to hemodynamics, mitral flow velocity and left atrial volume, and ejection fraction. J Am Soc Echocardiogr 1991;4:547–58.
8. Simek CL, Feldman MD, Haber HL, Wu CC, Jayaweera AR, Kaul S. Relationship between left ventricular wall thickness and left atrial size: comparison with other measures of diastolic function. J Am Soc Echocardiogr 1995;8:37–47.
9. Moller JE, Hillis GS, Oh JK, Seward JB, Reeder GS, Wright RS, et al. Left atrial volume: a powerful predictor of survival after acute myocardial infarction. Circulation 2003;107:2207–12.
10. McKee P, Castelli W, McNamara PM, Kannel WB. The natural history of congestive heart failure: the Framingham Study. N Engl J Med 1971;285:1441–6.
11. Arimoto T, Takeishi Y, Shiga R, Fukui A, Tachibana H, Nozaki N, et al. Prognostic value of elevated circulating heart-type fatty acid binding protein in patients with congestive heart failure. J Card Fail 2005;11:56–60.
12. Wang Y, Gutman JM, Heilbron D, Wahr D, Schiller NB. Atrial volume in a normal adult population by two-dimensional echocardiography. Chest 1984;86:595–601.
13. Abhayaratna WP, Seward JB, Appleton CP, Douglas PS, Oh JK, Tajik AJ, et al. Left atrial size: physiologic determinants and clinical applications. J Am Coll Cardiol 2006;47:2357–63.
14. Lang RM, Bierig M, Devereux RB, Flachskampf FA, Foster E, Pellikka PA, et al, American Society of Echocardiography's Guidelines and Standards Committee, European Association of Echocardiography. Recommendations for chamber quantification: a report from the American Society of Echocardiography's Guidelines and Standards Committee and the Chamber Quantification Writing Group, developed in conjunction with the European Association of Echocardiography, a branch of the European Society of Cardiology. J Am Soc Echocardiogr 2005;18:1440–63.
15. Devereux RB, Alonso DR, Lutas EM, Gottlieb GJ, Campo E, Sachs I, et al. Echocardiographic assessment of left ventricular hypertrophy: comparison to necropsy findings. Am J Cardiol 1986;57:450–8.
16. Tei C. New noninvasive index for combined systolic and diastolic ventricular function. J Cardiol 1995;26:135–6.
17. Niizeki T, Takeishi Y, Arimoto T, Takabatake N, Nozaki N, Hirono O, et al. Heart-type fatty acid–binding protein is more sensitive than troponin T to detect the ongoing myocardial damage in chronic heart failure patients. J Card Fail 2007;13:120–7.
18. Dent CL, Bowman AW, Scott MJ, Allen JS, Lisauskas JB, Janif M, et al. Echocardiographic characterization of fundamental mechanisms of abnormal diastolic filling in diabetic rats with a parameterized diastolic filling formalism. J Am Soc Echocardiogr 2001;14:1166–72.
19. Vasan RS, Larson MG, Benjamin EJ, Evans JC, Reiss CK, Levy D. Congestive heart failure in subjects with normal versus reduced left ventricular ejection fraction: prevalence and mortality in a population-based cohort. J Am Coll Cardiol 1999;33:1948–55.
20. Devereux RB, Roman MJ, Liu JE, Welty TK, Lee ET, Rodeheffer R, et al. Congestive heart failure despite normal left ventricular systolic function in a population-based sample: the Strong Heart Study. Am J Cardiol 2000;86:1090–6.
21. Kitzman DW, Gardin JM, Gottdiener JS, Arnold A, Boineau R, Aurigemma G, et al, CHS Research Group. Importance of heart failure with preserved systolic function in patients ≥65 years of age. Cardiovascular Health Study. Am J Cardiol 2001;87:413–9.
22. Owan TE, Hodge DO, Herges RM, Jacobsen SJ, Roger VL, Redfield MM. Trends in prevalence and outcome of heart failure with preserved ejection fraction. N Engl J Med 2006;355:251–9.

23. Tsang TS, Barnes ME, Gersh BJ, Bailey KR, Seward JB. Left atrial volume as a morphophysiologic expression of left ventricular diastolic dysfunction and relation to cardiovascular risk burden. Am J Cardiol 2002;90:1284–9.
24. Okura H, Kubo T, Asawa K, Toda I, Yoshiyama M, Yoshikawa J, et al. Elevated E/E′ predicts prognosis in congestive heart failure patients with preserved systolic function. Circ J 2009;73:86–91.
25. Valle R, Aspromonte N, Giovinazzo P, Carbonieri E, Chiatto M, di Tano G, et al. B-type natriuretic peptide–guided treatment for predicting outcome in patients hospitalized in sub-intensive care unit with acute heart failure. J Card Fail 2008;14:219–24.
26. Popescu BA, Popescu AC, Antonini-Canterin F, Rubin D, Cappelletti P, Piazza R, et al. Prognostic role of left atrial volume in elderly patients with symptomatic stable chronic heart failure: comparison with left ventricular diastolic dysfunction and B-type natriuretic peptide. Echocardiography 2007;24:1035–43.
27. Lim TK, Dwivedi G, Hayat S, Majumdar S, Senior R. Independent value of left atrial volume index for the prediction of mortality in patients with suspected heart failure referred from the community. Heart 2009;95:1172–8.
28. Nijland F, Kamp O, Karreman AJ, van Eenige MJ, Visser CA. Prognostic implications of restrictive left ventricular filling in acute myocardial infarction: a serial Doppler echocardiographic study. J Am Coll Cardiol 1997;30:1618–24.
29. Møller JE, Søndergaard E, Poulsen SH, Egstrup K. Pseudonormal and restrictive filling patterns predict left ventricular dilation and cardiac death after a first myocardial infarction: a serial color M-mode Doppler echocardiographic study. J Am Coll Cardiol 2000;36:1841–6.
30. Cerisano G, Bolognese L, Buonamici P, Valenti R, Carrabba N, Dovellini EV, et al. Prognostic implications of restrictive left ventricular filling in reperfused anterior acute myocardial infarction. J Am Coll Cardiol 2001;37:793–9.

Circulation Journal
Official Journal of the Japanese Circulation Society
http://www.j-circ.or.jp

ORIGINAL ARTICLE
Heart Failure

Prognostic Impact of Myocardial Interstitial Fibrosis in Non-Ischemic Heart Failure

– Comparison Between Preserved and Reduced Ejection Fraction Heart Failure –

Tatsuo Aoki, MD; Yoshihiro Fukumoto, MD, PhD; Koichiro Sugimura, MD, PhD; Minako Oikawa, MD, PhD; Kimio Satoh, MD, PhD; Makoto Nakano, MD, PhD; Masaharu Nakayama, MD, PhD; Hiroaki Shimokawa, MD, PhD

Background: Although myocardial fibrosis plays an important role in the progression of heart failure (HF), its prognostic impact still remains to be clarified.

Methods and Results: A total of 172 consecutive patients with chronic HF, who underwent cardiac catheterization and endomyocardial biopsy between January 2001 and September 2008, were examined. They were divided into 2 groups: HF with preserved ejection fraction (HFPEF; left ventricular ejection fraction [LVEF] ≥50%, n=81); and HF with reduced LVEF (HFREF; LVEF <50%, n=91). The collagen volume fraction (CVF) in biopsy samples was calculated and its prognostic impact examined. Mean follow-up in the HFPEF and the HFREF groups was 41± 33 months and 41±26 months, respectively. Although CVF was similar between the 2 groups (1.83±1.54% vs. 2.07± 2.35%), CVF was significantly correlated with LV end-diastolic pressure in the HFREF group but not in the HFPEF group. When HF stage was adjusted, the long-term prognosis was comparable between the 2 groups. When the patients were divided into 2 groups according to median CVF, however, severe fibrosis was a significant predictor for all-cause death (P=0.014) and cardiac events (P=0.02) in the HFREF, but not in the HFPEF group.

Conclusions: Myocardial fibrosis evaluated on biopsy samples is a useful indicator for long-term survival, suggesting that it may be an important therapeutic target as well. (*Circ J* 2011; **75:** 2605–2613)

Key Words: Collagen volume fraction; Ejection fraction; Fibrosis; Heart failure; Prognosis

Myocardial extracellular matrix (ECM) plays an important role in maintaining the structure of myocytes and blood vessels to strengthen myocardial tissue.[1,2] Myocardial collagen is the major constituent of ECM, and myocardial collagen volume is an important determinant of ventricular remodeling that affects ventricular functions.[3] It has previously been demonstrated that myocardial collagen content is correlated with left ventricular (LV) stiffness in patients with heart failure (HF),[4,5] and that the extent of myocardial collagen is correlated with a reduction in LV ejection fraction (LVEF) and is involved in the process of LV dilatation and progression of HF.[6,7] Furthermore, the presence of excessive collagen fibers may induce fatal ventricular arrhythmia.[8] Thus, it is important to estimate the extent of myocardial interstitial fibrosis in order to determine prognosis in HF patients.

Cardiovascular magnetic resonance imaging (MRI) is a useful tool to evaluate myocardial fibrosis that can be used to estimate the prognosis of HF patients by evaluation of LV midwall fibrosis using late gadolinium enhancement.[9] Indeed, MRI can detect and quantify regional myocardial fibrosis in a ventricle but not diffuse myocardial fibrosis.[10] Although serum levels of collagen synthesis markers (eg, procollagen type III amino-terminal peptide, PIIINP) may be useful to estimate the prognosis of HF patients,[11–13] those markers may reflect systemic fibrosis.[14,15] Indeed, little is known about the relationship between the prognosis of HF patients and the extent of myocardial fibrosis calculated directly from biopsy specimens in HF patients. In the present study, we thus examined whether collagen volume fraction (CVF) obtained from LV endomyocardial biopsy samples has a prognostic impact in HF patients with or without systolic dysfunction.

Received June 3, 2011; revised manuscript received June 23, 2011; accepted July 1, 2011; released online August 6, 2011 Time for primary review: 5 days

Department of Cardiovascular Medicine, Tohoku University Graduate School of Medicine, Sendai, Japan

The Guest Editor for this article was Masafumi Kitakaze, MD.

Mailing address: Yoshihiro Fukumoto, MD, PhD, Department of Cardiovascular Medicine, Tohoku University Graduate School of Medicine, 1-1 Seiryo-machi, Aoba-ku, Sendai 980-8575, Japan. E-mail: fukumoto@cardio.med.tohoku.ac.jp

ISSN-1346-9843 doi:10.1253/circj.CJ-11-0568

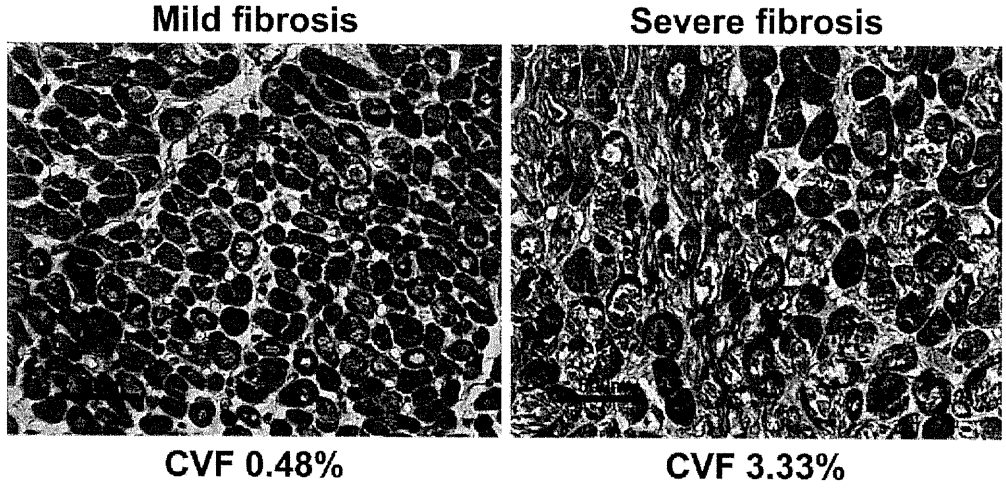

Figure 1. Representative histology of the (**Left**) mild and (**Right**) severe fibrosis groups. Myocardial fibrosis, stained in blue by Elastica–Masson staining. CVF, collagen volume fraction. Scale bar, 50 μm.

Methods

The ethics committees of Tohoku University Hospital approved the study protocol and all patients provided written informed consent.

Subjects

We examined 172 consecutive patients with chronic HF enrolled in the Tohoku University Hospital database, and who underwent cardiac catheterization and endomyocardial biopsy to determine the etiology of HF between January 2001 and September 2008. We performed endomyocardial biopsy in all HF patients with suspected cardiomyopathy but we did not perform the procedure in those who had apparent ischemic or valvular heart disease documented on echocardiography and/or cardiac catheterization.

For each patient, we collected clinical, hemodynamic, biochemistry and prognostic data and analyzed endomyocardial biopsy samples.

Definition of HF

In the present study, we included patients in stage B, C and D, according to the chronic HF ACC/AHA 2005 guidelines. According to the ESC 2007 HF guideline, we also divided them into 2 groups: HF with preserved ejection fraction (HFPEF; LVEF ≥50%, n=81) and HF with reduced LVEF (HFREF; LVEF <50%, n=91).

Data Collection

Baseline demographic data, hemodynamic data obtained via catheterization, stage of HF, medications and comorbidities (hypertension, diabetes mellitus, hyperlipidemia, and atrial fibrillation) were obtained based on medical records. The hemodynamic parameters measured via cardiac catheterization included LVEF, LV end-diastolic volume index (LVEDVI), mean aortic pressure, LV end-diastolic pressure (LVEDP), mean pulmonary artery pressure, pulmonary capillary wedge pressure (PCWP) and cardiac index. Before cardiac catheterization, we measured serum levels of hemoglobin, brain natriuretic peptide (BNP), creatinine and high-sensitivity C-reactive protein and estimated creatinine clearance using the Cockroft-Gault formula.

The primary endpoints included all-cause death, and the secondary combined endpoints included cardiovascular death, sudden death and admission for worsening of HF. Follow-up data were obtained from the database.

Quantitative Morphometry of Biopsy Samples

Trans-venous endomyocardial biopsy samples were obtained from the interventricular septum using 6-Fr Biotom (Cordis, Bridgewater, NJ, USA). There were no major complications related to the procedures during the study period. The tissues were immediately fixed in 10% buffered formalin and embedded in paraffin. Tissue sections were stained with hematoxylin–eosin and Elastica–Masson. Images of these sections were acquired with a projection microscope (×400; **Figure 1**). Subsequent image analysis was performed using Macscope 2.5 (Mitani, Fukui, Japan) to determine cardiomyocyte diameter and extent of myocardial interstitial fibrosis, which was expressed as CVF (%). CVF was calculated as the sum of all connective tissue areas divided by the sum of all connective tissue and muscle areas averaged over 2–5 representative fields of the section (mean, 3.6±0.9 fields), where there was no endocardium or blood vessel.[16,17] Myocardial diameter was determined at the nucleus level in 8–15 representative cardiomyocytes (mean, 12.0±2.5 fields) per section, where we also counted the number of inflammatory mononuclear cells in the same fields (mean, 6.0±1.8). This histological evaluation was performed by a well-trained cardiologist without knowledge of which patient provided the tissue sections.

We divided both the HFPEF and HFREF groups into 2 groups using median CVF (HFPEF and HFREF, 1.36% and 1.34%, respectively). We defined mild and severe fibrosis as CVF smaller and greater than the median, respectively (**Figure 1**).

Statistical Analysis

Continuous variables are expressed as mean±SD. Comparisons between 2 groups were conducted using unpaired t-test for continuous variables and chi-squared test for categorical

Table 1. Baseline Subject Characteristics

	HFPEF (n=81)	HFREF (n=91)	P value
Age (years)	54.3±14.1	55.9±12.8	0.429
BMI (kg/m²)	23.4±4.5	23.9±4.2	0.408
Male	54 (67)	66 (73)	0.404
Hypertension	34 (42)	39 (43)	0.962
Diabetes mellitus	9 (11)	13 (14)	0.533
Dyslipidemia	21 (26)	21 (23)	0.631
Sinus rhythm	69 (85)	65 (71)	0.028*
Medication			
ACEI	36 (44)	57 (63)	0.017*
ARB	15 (19)	35 (38)	0.004*
β-blocker	39 (48)	66 (73)	0.001*
Diuretics	13 (16)	41 (45)	<0.001*
Spironolactone	10 (12)	31 (34)	0.001*
Warfarin	12 (15)	46 (51)	<0.001*
Digitalis	7 (9)	28 (31)	<0.001*
CCB	26 (32)	11 (12)	0.001*
Antiplatelet	13 (16)	27 (30)	0.033*
Statin	7 (9)	17 (19)	0.054
Amiodarone	5 (6)	8 (9)	0.514
Stage of heart failure			<0.001*
B	40 (49)	15 (16)	
C	39 (48)	68 (75)	
D	2 (2)	8 (9)	
Laboratory data			
Hemoglobin (g/dl)	13.8±2.0	14.1±1.8	0.277
hsCRP (mg/dl)	0.21±0.46	0.33±0.93	0.294
BNP (pg/ml)	248±342	367±491	0.089
LDL (mg/dl)	110±41	121±39	0.103
HDL (mg/dl)	54.9±24.0	45.1±12.8	0.001*
TG (mg/dl)	131±98	137±75	0.669
Glucose (mg/dl)	106±37	106±21	0.934
CCr (ml/min)	90.1±25.1	88.2±35.4	0.694
Hemodynamic data			
LVEDVI (ml/m²)	75.7±20.4	114.5±35.1	<0.001*
EF (%)	67.8±11.3	35.6±11.0	<0.001*
mAoP (mmHg)	96±15	90±17	0.023*
LVEDP (mmHg)	14±6	13±7	0.420
mPAP (mmHg)	16.7±4.8	19.9±7.7	0.002*
PCWP (mmHg)	9.5±4.2	11.2±6.5	0.050
Cardiac index ($L \cdot min^{-1} \cdot m^{-2}$)	2.9±0.7	2.6±0.7	0.021*
Morphometric data			
CVF (%)	1.83±1.54	2.07±2.35	0.440
MyD (μm)	19.2±3.2	19.7±2.8	0.362
Inflammatory cell (/field)	4.9±4.9	7.0±6.0	0.015*
All-cause death	0 (0)	9 (10)	0.004*
Cardiac events	4 (5)	15 (16)	0.016*
Cardiac or sudden death	0 (0)	4 (4)	
Admission for HF	4 (5)	11 (12)	

Data given as mean±SD or n (%). *P<0.05, HFPEF vs. HFREF.
HFPEF, heart failure patients with preserved left ventricular ejection fraction; HFREF, heart failure patients with reduced left ventricular ejection fraction; BMI, body mass index; ACEI, angiotensin-converting enzyme inhibitor; ARB, angiotensin receptor blocker; CCB, calcium cannel blocker; hsCRP, high-sensitivity C-reactive protein; BNP, brain natriuretic peptide; LDL, low-density lipoprotein; HDL, high-density lipoprotein; CCr, creatinine clearance; LVEDVI, left ventricular end-diastolic volume index; EF, ejection fraction; mAoP, mean aortic pressure; LVEDP, left ventricular end-diastolic pressure; mPAP, mean pulmonary artery pressure; PCWP, pulmonary capillary wedge pressure; CVF, collagen volume fraction; MyD, cardiomyocyte diameter; HF, heart failure.

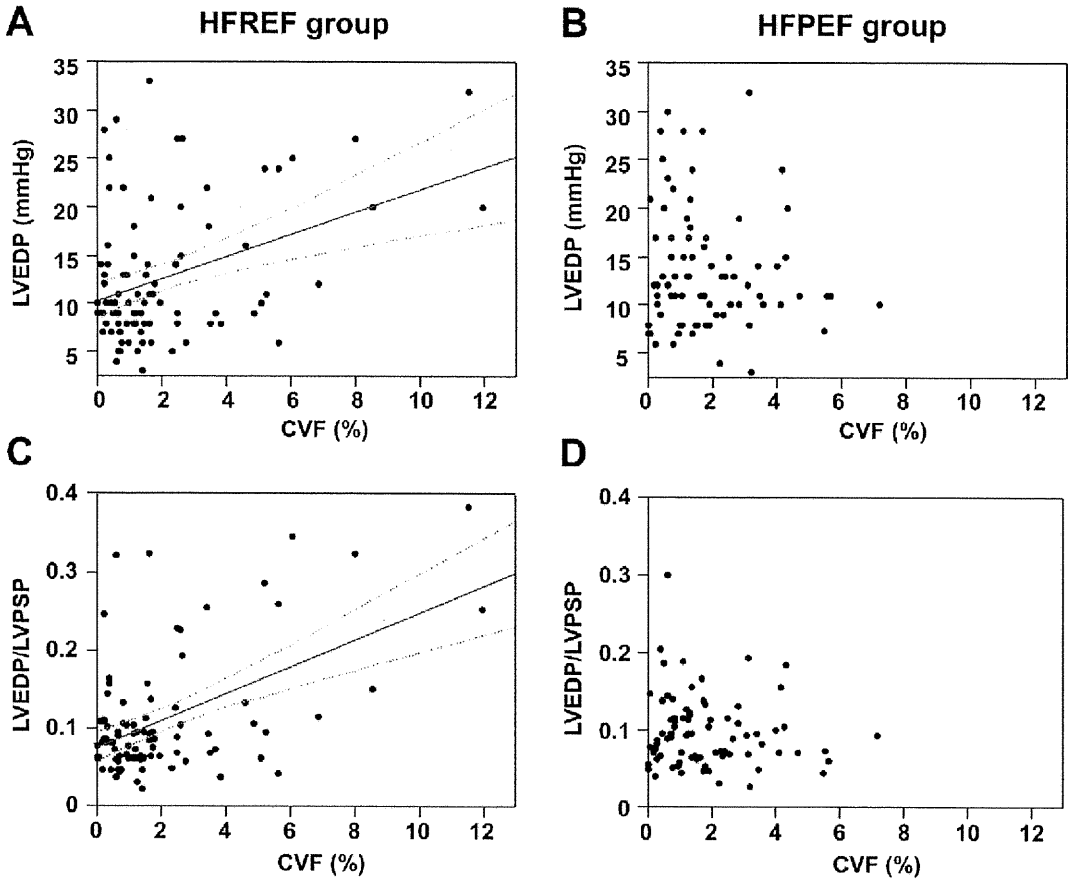

Figure 2. Correlation between left ventricular end-diastolic pressure (LVEDP) and collagen volume fraction (CVF). (**A**) A significant correlation was noted between CVF and LVEDP for patients with heart failure (HF) with reduced left ventricular ejection fraction (HFREF; r=0.387, P<0.001) but not for those with (**B**) HF with preserved left ventricular ejection fraction (HFPEF; r=–0.092, P=0.664). (**C**) LVEDP/left ventricular peak systolic pressure (LVEDP/LVPSP) ratio and CVF were also significantly correlated in the HFREF group (r=0.515, P<0.001), but not in the (**D**) HFPEF group (r=–0.097, P=0.393).

variables. For echocardiographic comparison before and after medical treatment, paired t-test was used. Five-year survival free from all-cause death and that from cardiac events was estimated using the Kaplan-Meier method. We used Cox proportional hazards model to adjust covariates. After comparison of covariates between the mild and severe fibrosis groups, the covariates with P<0.05 were used in the final multivariate models. Furthermore, we evaluated the prognostic value of CVF as a continuous variable. We used the variables with P<0.05 on univariate analysis in the final multivariate models, in which age, cardiac index, LV filling pressure, and stage of HF were controlled for, and we chose the parameters for final models using the step-up method. In these analyses, we used PCWP as a parameter of LV filling pressure, because LVEDP data were lacking in 3 cases. Furthermore, as previously reported,[18] we tested the proportionality assumptions of each parameter of the final models, with P<0.05 indicating non-proportionality. All statistical analysis was performed using JMP 7.0.2 (SAS Institute, Cary, NC, USA) and R 2.8.1(www.r-project.org/). All P-values were 2-sided, and P<0.05 was considered to be statistically significant.

Results

HFPEF Group vs. HFREF Group

All patients were successfully followed up in the present study. Mean follow-up period in the HFPEF and the HFREF groups was 41±33 months and 41±26 months, respectively. The HFREF group was characterized by more advanced stage of HF (**Table 1**). There were more all-cause deaths and cardiac events in the HFREF group than in the HFPEF group (**Table 1**). Five-year prognosis was significantly lower in the HFREF group than in the HFPEF group, in terms of survival from all-cause death (P=0.006) and survival from cardiac events (P=0.034). After the adjustment of HF stage of HF, however, there was no significant difference in cardiac events between the 2 groups.

The prevalence of the use of medications for HF at cardiac catheterization, including angiotensin-converting enzyme inhibitors (ACEI), angiotensin receptor blockers (ARB), β-blockers, diuretics, spironolactone and digitalis, was significantly higher in the HFREF than in the HFPEF group (**Table 1**). In contrast, the use of calcium cannel blockers (CCB) was more common in the HFPEF group (**Table 1**). The HFREF group had significantly larger LV volume, lower LVEF and lower cardiac index compared with the HFPEF group

Table 2. Subject Characteristics vs. Level of Fibrosis

	HFPEF			HFREF		
	Mild fibrosis (n=40)	Severe fibrosis (n=41)	P value	Mild fibrosis (n=46)	Severe fibrosis (n=45)	P value
Age (years)	57±11	52±16	0.082	58±12	54±14	0.21
BMI (kg/m²)	23±5	23±4	0.96	24±4	24±4	0.372
Male	29 (73)	25 (63)	0.238	34 (74)	32 (70)	0.949
Hypertension	13 (33)	21 (53)	0.164	21 (46)	18 (39)	0.739
Diabetes mellitus	5 (13)	4 (10)	0.906	5 (11)	8 (17)	0.521
Dyslipidemia	10 (25)	11 (28)	0.894	12 (26)	9 (20)	0.66
Sinus rhythm	31 (78)	38 (93)	0.281	31 (67)	34 (76)	0.389
Medication						
ACEI	17 (43)	19 (48)	0.941	28 (61)	29 (63)	0.892
ARB	7 (18)	8 (20)	0.874	18 (39)	17 (37)	0.934
β-blocker	19 (48)	20 (50)	0.902	32 (70)	34 (74)	0.685
Diuretics	7 (18)	6 (15)	0.884	17 (37)	24 (52)	0.174
Spironolactone	7 (18)	3 (8)	0.255	16 (35)	15 (33)	0.94
Warfarin	5 (13)	7 (18)	0.862	20 (43)	26 (57)	0.248
Digitalis	5 (13)	2 (5)	0.371	17 (37)	11 (24)	0.287
CCB	14 (35)	12 (30)	0.64	6 (13)	5 (11)	0.969
Antiplatelet	6 (15)	7 (18)	0.884	14 (30)	13 (28)	0.946
Statin	2 (5)	5 (13)	0.491	8 (17)	9 (20)	0.96
Amiodarone	5 (13)	0 (0)	0.053	3 (7)	5 (11)	0.687
Stage of heart failure			0.236			0.577
B	23 (58)	17 (43)		9 (20)	6 (13)	
C	16 (40)	23 (58)		34 (74)	34 (74)	
D	1 (3)	1 (3)		3 (7)	5 (11)	
Laboratory data						
Hemoglobin (g/dl)	14±2	14±2	0.357	14±2	14±2	0.674
hsCRP (mg/dl)	0.16±0.29	0.26±0.58	0.317	0.35±1.12	0.32±0.69	0.888
BNP (pg/ml)	255±377	243±314	0.892	245±347	494±584	0.019*
LDL (mg/dl)	108±38	113±44	0.635	116±38	125±40	0.239
HDL (mg/dl)	52±21	58±26	0.269	45±14	45±11	0.952
TG (mg/dl)	125±75	137±116	0.603	145±86	129±62	0.305
Glucose mg/dl)	112±43	100±29	0.134	104±19	109±23	0.315
CCr (ml/min)	90±25	90±26	0.898	89±30	87±40	0.804
Hemodynamic data						
LVEDVI (ml/m²)	76±18	75±22	0.874	107±28	122±40	0.040*
EF (%)	66±11	69±11	0.275	38±11	33±11	0.053
mAoP (mmHg)	97±16	96±15	0.775	92±15	88±19	0.189
LVEDP (mmHg)	14±7	13±6	0.236	11±6	14±8	0.06
mPAP (mmHg)	17±4	17±5	0.736	19±7	21±9	0.136
PCWP (mmHg)	10±4	9±4	0.926	10±5	12±8	0.161
Cardiac index (L·min⁻¹·m⁻²)	2.9±0.7	2.9±0.7	0.932	2.7±0.7	2.6±0.6	0.367
Morphometric data						
CVF (%)	0.64±0.41	2.93±1.38	<0.001*	0.61±0.4	3.56±2.58	<0.001*
MyD (μm)	19±1.9	20±4.1	0.287	19±2	20±3	0.055
Inflammatory cell (/field)	4.7±4.6	5.1±5.2	0.696	8±6	6±6	0.116
All-cause death	0 (0)	0 (0)	–	1 (2)	8 (18)	0.013*
Cardiac events	3 (8)	1 (2)	0.293	3 (7)	12 (27)	0.001*
Cardiac or sudden death	0 (0)	0 (0)		1 (2)	3 (7)	
Admission for HF	3 (8)	1 (2)		2 (4)	9 (20)	

Data given as mean±SD or n (%). *P<0.05, mild fibrosis vs. severe fibrosis.
Abbreviations see in Table 1.

(Table 1). Although LVEDP and CVF were comparable between the 2 groups (Table 1), CVF was significantly correlated with LVEDP, and also with LV peak systolic pressure (LVPSP) after adjustment in the HFREF group (Figures 2A,C), but not in the HFPEF group (Figures 2B,C).

Morphometric Variables as Prognostic Indicators

When comparing the mild and the severe fibrosis groups, a statistically significant difference was noted in terms of LVEDVI and BNP in the HFREF group (Table 2), but not in the HFPEF group (Table 2).

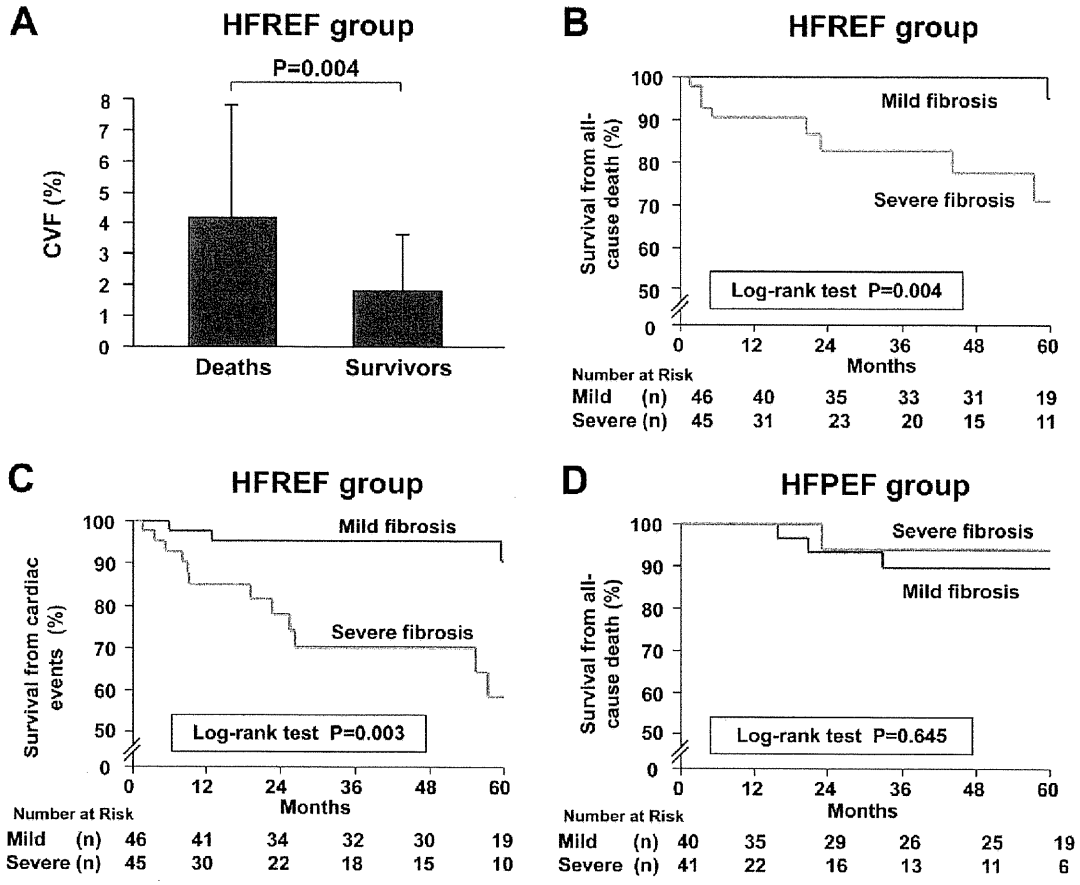

Figure 3. Comparison of survival between the mild and the severe fibrosis groups. (**A**) Collagen volume fraction (CVF) was significantly higher in heart failure (HF) patients who died than in survivors. (**B**,**C**) The mild fibrosis group had better survival from (**B**) all-cause death and (**C**) cardiac events compared with the severe fibrosis group. (**D**) In contrast, no difference was noted between the mild and severe fibrosis groups. HFPEF, heart failure patients with preserved left ventricular ejection fraction; HFREF, heart failure patients with reduced left ventricular ejection fraction.

In the HFREF group, CVF was significantly higher in HF patients who died than in survivors (**Figure 3A**). Indeed, there were more all-cause deaths and cardiac events in the severe fibrosis group than in the mild fibrosis group (**Table 2**). Five-year survival from all-cause death was significantly lower in the severe fibrosis group than in the mild fibrosis group (P=0.004; **Figure 3B**), and was so even after adjustment with the covariate (severe fibrosis vs. mild fibrosis; hazard ratio [HR], 13.5; 95% confidence interval [CI]: 2.01–307, P=0.006). Similarly, survival after cardiac events was significantly lower in the severe fibrosis group than in the mild fibrosis group in the HFREF subjects (P=0.003; **Figure 3C**), and was so even after adjustment with the covariate (severe fibrosis vs. mild fibrosis; HR, 6.20; 95%CI: 1.52–25.4, P=0.011). In contrast, in the HFPEF group, there was no significant difference in the cardiac events (**Table 1**) or survival rate (**Figure 3D**) between the mild and severe fibrosis groups. In the HFREF group, multivariate analysis showed that a 1% elevation of CVF increased the risk of all-cause death and that of cardiac events by 1.50-fold (95%CI: 1.18–1.95, P=0.002) and 1.28-fold (95%CI: 1.07–1.50, P=0.008), respectively (**Figure 4**). Furthermore, other histological parameters (eg, cardiomyocyte hypertrophy) were not significant predictors in the present study.

Discussion

The novel findings of the present study are as follows: (1) CVF was similar between the HFPEF and HFREF groups; (2) CVF was an independent predictor of all-cause death and cardiac events in the HFREF group but not in the HFPEF group; and (3) CVF was significantly correlated with LVEDP in the HFREF group but not in the HFPEF group. To the best of our knowledge, this is the first report to demonstrate the prognostic impact of CVF in non-ischemic HF patients with systolic dysfunction.

HFPEF Group vs. HFREF Group

Several studies have shown that the prognosis is comparable between patients with HFPEF and those with HFREF.[19–21] In the present study, the patients with HFPEF had a significantly better prognosis than those with HFREF, but after adjustment for stage of HF, the survival became similar between the 2 groups. In the present study, the 5-year survival rate from all-cause death was better than in the previous study,[22] probably because we followed up the patients monthly to control sodium intake and blood pressure. It has been reported that intensive medical treatment for HF patients with close fol-

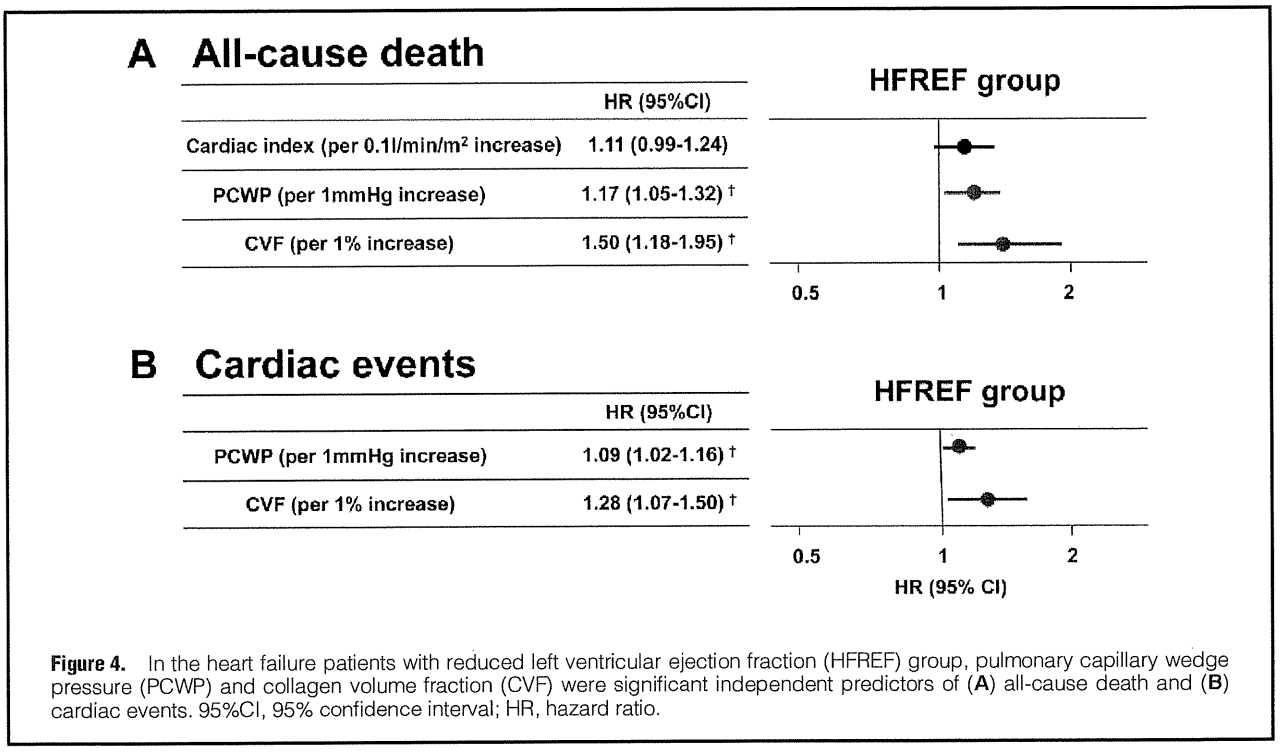

Figure 4. In the heart failure patients with reduced left ventricular ejection fraction (HFREF) group, pulmonary capillary wedge pressure (PCWP) and collagen volume fraction (CVF) were significant independent predictors of (**A**) all-cause death and (**B**) cardiac events. 95%CI, 95% confidence interval; HR, hazard ratio.

low-up can reduce re-admission for HF and cardiac deaths,[23] suggesting that the regular follow-up in the present study was effective to improve the prognosis of the HF patients.

Morphometric Variables and Cardiac Function as Prognostic Indicators

Myocardial fibrillar collagen, the main component of ECM, is a major contributor to myocardial stiffness.[3] In the present study, CVF in the HFPEF and the HFREF groups was 1.83% and 2.07%, respectively, consistent with the previous report.[24]

Recently, degradation of interstitial collagen has been reported in patients with mild to moderate dilated cardiomyopathy (DCM).[25,26] In contrast, marked accumulation of myocardial interstitial fibrosis has also been reported in patients with end-stage HFREF (eg, explanted heart).[27] The present study also demonstrated that CVF was significantly higher in HF patients who died than in survivors and that CVF and LVEDP were significantly correlated in HFREF patients. Taken together, these results suggest that reduction of myocardial interstitial collagen causes LV dilatation complicated with systolic dysfunction in the early stage of HFREF and that the increased myocardial interstitial collagen causes diastolic dysfunction in the advanced stage of HFREF with the resultant poor prognosis.

Although cardiac MRI is well established as a method for evaluating cardiac fibrosis, it cannot detect all cases of severe fibrosis, especially in HFREF patients with non-ischemic etiology.[28] It has also been reported that diffuse cardiac fibrosis is not able to be detected on cardiac MRI.[29] Furthermore, a recent study has shown that late gadolinium enhancement does not always indicate the change in myocardial interstitium.[30] Our preliminary data showed that there was no significant difference in CVF between the patients with and those without delayed enhancement on cardiac MRI (unpublished observation). Thus, we consider that the extent of myocardial fibrosis should be evaluated in multiple ways, including on endomyocardial biopsy, MRI and via serum markers of collagen turnover.

It has been reported that HFREF patients with diastolic dysfunction had a worse prognosis than those without it.[31,32] In the present study, elevated LVEDP was significantly related to increased CVF. Therefore, accumulation of myocardial interstitial fibrillar collagen may have caused ventricular diastolic dysfunction in the HFREF group with a resultant poor prognosis. The Randomized Aldactone Evaluation Study (RALES) showed that spironolactone improves prognosis in HF patients.[33] Interestingly, the RALES subanalysis showed that this benefit of spironolactone is noted only in patients with a high level of collagen synthesis marker (PIIINP) but not in those with low PIIINP.[11,33] It has also been shown that spironolactone reduced LV diastolic dysfunction only in DCM patients with increased myocardial fibrosis.[34]

In contrast, HFPEF seems to be a very different condition from HFREF in terms of response to medical treatment. Although ARB and ACEI could decrease myocardial fibrosis in HFPEF,[4,35,36] large clinical trials failed to demonstrate any beneficial effects of ARB or ACEI (eg, irbesartan, candesartan, enalapril, and valsartan) in patients with HFPEF.[37–40] This is consistent with the present finding that no significant correlation was noted between myocardial fibrosis and cardiac events in the HFPEF group, suggesting that the prognostic impact of myocardial fibrosis might be small in HFPEF. It has been previously reported, however, that in approximately 20% of patients with HFPEF, LVEF was significantly decreased during the 3-month follow-up period,[41] which is consistent with the present study, in which LVEF was significantly decreased in 11% of patients with HFPEF during follow-up. Thus, patients with severe myocardial fibrosis should be closely followed up because HFPEF patients with large CVF are at higher risk for disease progression and poor prognosis.

CVF and LVEDP

In the present study a significant but relatively weak correlation was noted between CVF and LVEDP in the HFREF group, probably because 60–70% of the HFREF patients received β-blockers and ACEI and/or ARB, which might have affected the systemic hemodynamics measured during cardiac catheterization.

As mentioned here, we were unable to observe any significant correlation between CVF and LVEDP in the HFPEF group, probably because the HFPEF is associated with heterogeneous diseases, such as hypertensive heart disease, cardiac amyloidosis, early-stage DCM and hypertrophic cardiomyopathy, and could also have been affected by the medical treatment including β-blocker and ACEI and/or ARB.

Study Limitations

Several limitations should be mentioned for the present study. First, we assessed only the collagen content in the myocardium. It was previously reported that not only the quantity but also the quality of collagen are important determinants for myocardial stiffness.[42] Indeed, the ratio of cross-linked collagen (insoluble collagen) to non-cross-linked collagen (soluble collagen) and the type I/type III collagen ratio are important determinants of myocardial stiffness,[17,27,43] and reduction in collagen cross-linking ameliorates myocardial stiffness and ventricular dilatation irrespective of collagen content.[44] Although we did not measure collagen turnover markers that have been established as prognostic in HF patients, it has been reported that there is a significant correlation between CVF and procollagen I carboxy-terminal peptide (PICP), a collagen synthesis marker.[45] Thus, the quality of ventricular fibrosis should be evaluated in biopsy specimens in future studies.

Second, because myocardial fibrosis may exist in a patchy fashion, we obtained at least 3 endomyocardial biopsy samples in each patient and evaluated CVF in as many fields as possible (mean, 3.6±0.9 fields) in order to minimize errors from patchy distribution of myocardial fibrosis in the present study. We still consider that we should evaluate the extent of myocardial fibrosis in multiple ways, including on endomyocardial biopsy, MRI and via serum markers of collagen turnover.

Third, in the present study, the HF subject group might be biased because we included patients who underwent endomyocardial biopsy alone and excluded those with other major causes of HF, such as ischemic heart disease and valvular heart disease. But because we did not include HF patients with valvular or ischemic etiology, we were able to minimize the overestimation of LVEF due to those factors in the present study.

Fourth, the present study was an observational study with a relatively small number of patients, and for reasons of ethics we were unable to perform repetitive myocardial biopsy to evaluate the time-course of HF. Thus, a future study with a large number of patients with a longer follow-up is required to address this issue.

Finally, the relatively small number of events limits the generalization of the present findings. Although we analyzed the present results with several statistical models, we found that the Cox proportional hazard model was the best. Thus, after univariate analysis, we used the Cox proportional hazard model with as small covariates as possible.

In conclusion, we have demonstrated that myocardial CVF evaluated with biopsy samples is a useful predictor for long-term survival in patients with HFREF (but not in those with HFPEF), and may be an important therapeutic target as well.

Acknowledgments

We thank Shizuka Osaki and Goh Kato for their valuable technical contribution to this study. This work was supported by grants-in-aid (Nos. 15256003, 16209027, 16659192, 19590803, and 21590884) from the Japanese Ministry of Education, Culture, Sports, Science and Technology, Tokyo, Japan and from the Japanese Ministry of Health, Labour, and Welfare, Tokyo, Japan (Nos. 08005713, 09158526).

Disclosures

None.

References

1. Janicki J, Brower G. The role of myocardial fibrillar collagen in ventricular remodeling and function. *J Card Fail* 2002; **8**(Suppl): S319–S325.
2. Fukumoto Y, Deguchi J, Libby P, Rabkin-Aikawa E, Sakata Y, Chin M, et al. Genetically determined resistance to collagenase action augments interstitial collagen accumulation in atherosclerotic plaques. *Circulation* 2004; **110:** 1953–1959.
3. Borbély A, van der Velden J, Papp Z, Bronzwaer J, Edes I, Stienen G, et al. Cardiomyocyte stiffness in diastolic heart failure. *Circulation* 2005; **111:** 774–781.
4. Díez J, Querejeta R, López B, González A, Larman M, Martínez Ubago J. Losartan-dependent regression of myocardial fibrosis is associated with reduction of left ventricular chamber stiffness in hypertensive patients. *Circulation* 2002; **105:** 2512–2517.
5. van Heerebeek L, Hamdani N, Handoko M, Falcao-Pires I, Musters R, Kupreishvili K, et al. Diastolic stiffness of the failing diabetic heart: Importance of fibrosis, advanced glycation end products, and myocyte resting tension. *Circulation* 2008; **117:** 43–51.
6. Hein S, Arnon E, Kostin S, Schönburg M, Elsässer A, Polyakova V, et al. Progression from compensated hypertrophy to failure in the pressure-overloaded human heart: Structural deterioration and compensatory mechanisms. *Circulation* 2003; **107:** 984–991.
7. Graham H, Trafford A. Spatial disruption and enhanced degradation of collagen with the transition from compensated ventricular hypertrophy to symptomatic congestive heart failure. *Am J Physiol Heart* 2007; **292:** H1364–H1372.
8. Bello D, Fieno D, Kim R, Pereles F, Passman R, Song G, et al. Infarct morphology identifies patients with substrate for sustained ventricular tachycardia. *J Am Coll Cardiol* 2005; **45:** 1104–1108.
9. Assomull R, Prasad S, Lyne J, Smith G, Burman E, Khan M, et al. Cardiovascular magnetic resonance, fibrosis, and prognosis in dilated cardiomyopathy. *J Am Coll Cardiol* 2006; **48:** 1977–1985.
10. Jellis C, Martin J, Narula J, Marwick T. Assessment of nonischemic myocardial fibrosis. *J Am Coll Cardiol* 2010; **56:** 89–97.
11. Zannad F, Alla F, Dousset B, Perez A, Pitt B. Limitation of excessive extracellular matrix turnover may contribute to survival benefit of spironolactone therapy in patients with congestive heart failure: Insights from the Randomized Aldactone Evaluation Study (RALES): RALES Investigators. *Circulation* 2000; **102:** 2700–2706.
12. Cicoira M, Rossi A, Bonapace S, Zanolla L, Golia G, Franceschini L, et al. Independent and additional prognostic value of aminoterminal propeptide of type III procollagen circulating levels in patients with chronic heart failure. *J Card Fail* 2004; **10:** 403–411.
13. Braunwald E. Biomarkers in heart failure. *N Engl J Med* 2008; **358:** 2148–2159.
14. Soylemezoglu O, Wild G, Dalley AJ, MacNeil S, Milford-Ward A, Brown CB, et al. Urinary and serum type III collagen: Markers of renal fibrosis. *Nephrol Dial Transplant* 1997; **12:** 1883–1889.
15. Leroy V. Other non-invasive markers of liver fibrosis. *Gastroenterol Clin Biol* 2008; **32**(Suppl 1): 52–57.
16. van Heerebeek L, Borbély A, Niessen H, Bronzwaer J, van der Velden J, Stienen G, et al. Myocardial structure and function differ in systolic and diastolic heart failure. *Circulation* 2006; **113:** 1966–1973.
17. Fukui S, Fukumoto Y, Suzuki J, Saji K, Nawata J, Tawara S, et al. Long-term inhibition of Rho-kinase ameliorates diastolic heart failure in hypertensive rats. *J Cardiovasc Pharmacol* 2008; **51:** 317–326.
18. Tribouilloy C, Rusinaru D, Mahjoub H, Soulière V, Lévy F, Peltier M, et al. Prognosis of heart failure with preserved ejection fraction: A 5 year prospective population-based study. *Eur Heart J* 2008; **29:** 339–347.
19. Senni M, Redfield M. Heart failure with preserved systolic function: A different natural history? *J Am Coll Cardiol* 2001; **38:** 1277–1282.

20. Miyagishima K, Hiramitsu S, Kimura H, Mori K, Ueda T, Kato S, et al. Long term prognosis of chronic heart failure: Reduced vs preserved left ventricular ejection fraction. *Circ J* 2009; **73:** 92–99.
21. Tsuchihashi-Makaya M, Hamaguchi S, Kinugawa S, Yokota T, Goto D, Yokoshiki H, et al. Characteristics and outcomes of hospitalized patients with heart failure and reduced vs preserved ejection fraction: Report from the Japanese Cardiac Registry of Heart Failure in Cardiology (JCARE-CARD). *Circ J* 2009; **73:** 1893–1900.
22. Owan T, Hodge D, Herges R, Jacobsen S, Roger V, Redfield M. Trends in prevalence and outcome of heart failure with preserved ejection fraction. *N Engl J Med* 2006; **355:** 251–259.
23. Capomolla S, Febo O, Ceresa M, Caporotondi A, Guazzotti G, La Rovere M, et al. Cost/utility ratio in chronic heart failure: Comparison between heart failure management program delivered by day-hospital and usual care. *J Am Coll Cardiol* 2002; **40:** 1259–1266.
24. López B, González A, Querejeta R, Larman M, Díez J. Alterations in the pattern of collagen deposition may contribute to the deterioration of systolic function in hypertensive patients with heart failure. *J Am Coll Cardiol* 2006; **48:** 89–96.
25. Schwartzkopff B, Fassbach M, Pelzer B, Brehm M, Strauer B. Elevated serum markers of collagen degradation in patients with mild to moderate dilated cardiomyopathy. *Eur J Heart Fail* 2002; **4:** 439–444.
26. Timonen P, Magga J, Risteli J, Punnonen K, Vanninen E, Turpeinen A, et al. Cytokines, interstitial collagen and ventricular remodelling in dilated cardiomyopathy. *Int J Cardiol* 2008; **124:** 293–300.
27. Marijianowski M, Teeling P, Mann J, Becker A. Dilated cardiomyopathy is associated with an increase in the type I/type III collagen ratio: A quantitative assessment. *J Am Coll Cardiol* 1995; **25:** 1263–1272.
28. Bello D, Shah D, Farah G, Di Luzio S, Parker M, Johnson M, et al. Gadolinium cardiovascular magnetic resonance predicts reversible myocardial dysfunction and remodeling in patients with heart failure undergoing beta-blocker therapy. *Circulation* 2003; **108:** 1945–1953.
29. Iles L, Pfluger H, Phrommintikul A, Cherayath J, Aksit P, Gupta SN, et al. Evaluation of diffuse myocardial fibrosis in heart failure with cardiac magnetic resonance contrast-enhanced T1 mapping. *J Am Coll Cardiol* 2008; **52:** 1574–1580.
30. Yilmaz A, Kindermann I, Kindermann M, Mahfoud F, Ukena C, Athanasiadis A, et al. Comparative evaluation of left and right ventricular endomyocardial biopsy: Differences in complication rate and diagnostic performance. *Circulation* 2010; **122:** 900–909.
31. Bruch C, Gotzmann M, Stypmann J, Wenzelburger F, Rothenburger M, Grude M, et al. Electrocardiography and Doppler echocardiography for risk stratification in patients with chronic heart failure: Incremental prognostic value of QRS duration and a restrictive mitral filling pattern. *J Am Coll Cardiol* 2005; **45:** 1072–1075.
32. Whalley G, Doughty R, Gamble G, Wright S, Walsh H, Muncaster S, et al. Pseudonormal mitral filling pattern predicts hospital re-admission in patients with congestive heart failure. *J Am Coll Cardiol* 2002; **39:** 1787–1795.
33. Pitt B, Zannad F, Remme W, Cody R, Castaigne A, Perez A, et al. The effect of spironolactone on morbidity and mortality in patients with severe heart failure: Randomized Aldactone Evaluation Study Investigators. *N Engl J Med* 1999; **341:** 709–717.
34. Izawa H, Murohara T, Nagata K, Isobe S, Asano H, Amano T, et al. Mineralocorticoid receptor antagonism ameliorates left ventricular diastolic dysfunction and myocardial fibrosis in mildly symptomatic patients with idiopathic dilated cardiomyopathy: A pilot study. *Circulation* 2005; **112:** 2940–2945.
35. Brilla C, Funck R, Rupp H. Lisinopril-mediated regression of myocardial fibrosis in patients with hypertensive heart disease. *Circulation* 2000; **102:** 1388–1393.
36. Brilla C, Rupp H, Maisch B. Effects of ACE inhibition versus non-ACE inhibitor antihypertensive treatment on myocardial fibrosis in patients with arterial hypertension: Retrospective analysis of 120 patients with left ventricular endomyocardial biopsies. *Herz* 2003; **28:** 744–753.
37. Zile M, Gaasch W, Anand I, Haass M, Little W, Miller A, et al. Mode of death in patients with heart failure and a preserved ejection fraction: Results from the Irbesartan in Heart Failure With Preserved Ejection Fraction Study (I-Preserve) trial. *Circulation* 2010; **121:** 1393–1405.
38. Yusuf S, Pfeffer M, Swedberg K, Granger C, Held P, McMurray J, et al. Effects of candesartan in patients with chronic heart failure and preserved left-ventricular ejection fraction: The CHARM-Preserved Trial. *Lancet* 2003; **362:** 777–781.
39. Kitzman D, Hundley W, Brubaker P, Morgan T, Moore J, Stewart K, et al. A randomized, double-blinded trial of enalapril in older patients with heart failure and preserved ejection fraction: Effects on exercise tolerance and arterial distensibility. *Circ Heart Fail* 2010; **3:** 477–485.
40. Parthasarathy H, Pieske B, Weisskopf M, Andrews C, Brunel P, Struthers A, et al. A randomized, double-blind, placebo-controlled study to determine the effects of valsartan on exercise time in patients with symptomatic heart failure with preserved ejection fraction. *Eur J Heart Fail* 2009; **11:** 980–989.
41. Cahill J, Ryan E, Travers B, Ryder M, Ledwidge M, McDonald K. Progression of preserved systolic function heart failure to systolic dysfunction: A natural history study. *Int J Cardiol* 2006; **106:** 95–102.
42. Kass D, Bronzwaer J, Paulus W. What mechanisms underlie diastolic dysfunction in heart failure? *Circ Res* 2004; **94:** 1533–1542.
43. Badenhorst D, Maseko M, Tsotetsi O, Naidoo A, Brooksbank R, Norton G, et al. Cross-linking influences the impact of quantitative changes in myocardial collagen on cardiac stiffness and remodelling in hypertension in rats. *Cardiovasc Res* 2003; **57:** 632–641.
44. Woodiwiss A, Tsotetsi O, Sprott S, Lancaster E, Mela T, Chung E, et al. Reduction in myocardial collagen cross-linking parallels left ventricular dilatation in rat models of systolic chamber dysfunction. *Circulation* 2001; **103:** 155–160.
45. López B, González A, Varo N, Laviades C, Querejeta R, Díez J. Biochemical assessment of myocardial fibrosis in hypertensive heart disease. *Hypertension* 2001; **38:** 1222–1226.

Renal collecting duct epithelial cells regulate inflammation in tubulointerstitial damage in mice

Katsuhito Fujiu,[1,2] Ichiro Manabe,[1,3] and Ryozo Nagai[1,2,3,4]

[1]Department of Cardiovascular Medicine, [2]Translational Systems Biology and Medicine Initiative, [3]Global COE, and [4]Translational Research Center, the University of Tokyo Graduate School of Medicine, Tokyo, Japan.

Renal tubulointerstitial damage is the final common pathway leading from chronic kidney disease to end-stage renal disease. Inflammation is clearly involved in tubulointerstitial injury, but it remains unclear how the inflammatory processes are initiated and regulated. Here, we have shown that in the mouse kidney, the transcription factor Krüppel-like factor–5 (KLF5) is mainly expressed in collecting duct epithelial cells and that *Klf5* haploinsufficient mice (*Klf5*$^{+/-}$ mice) exhibit ameliorated renal injury in the unilateral ureteral obstruction (UUO) model of tubulointerstitial disease. Additionally, *Klf5* haploinsufficiency reduced accumulation of CD11b^{+}F4/80^{lo} cells, which expressed proinflammatory cytokines and induced apoptosis among renal epithelial cells, phenotypes indicative of M1-type macrophages. By contrast, it increased accumulation of CD11b^{+}F4/80^{hi} macrophages, which expressed CD206 and CD301 and contributed to fibrosis, in part via TGF-β production — phenotypes indicative of M2-type macrophages. Interestingly, KLF5, in concert with C/EBPα, was found to induce expression of the chemotactic proteins S100A8 and S100A9, which recruited inflammatory monocytes to the kidneys and promoted their activation into M1-type macrophages. Finally, assessing the effects of bone marrow–specific *Klf5* haploinsufficiency or collecting duct– or myeloid cell–specific *Klf5* deletion confirmed that collecting duct expression of *Klf5* is essential for inflammatory responses to UUO. Taken together, our results demonstrate that the renal collecting duct plays a pivotal role in the initiation and progression of tubulointerstitial inflammation.

Introduction

The incidence of end-stage renal disease is increasing worldwide and represents a growing clinical and economic burden. Regardless of whether renal injury begins in the glomeruli or within the tubulointerstitium, tubulointerstitial damage is a common feature of all chronic progressive renal diseases and is considered to be the final common pathway leading from chronic kidney disease to end-stage renal disease (1–3). In cases of chronic kidney disease, inflammation is a critical mechanism that promotes closely interlinked fibrosis and cellular injury within the tubulointerstitium (4), and macrophages are the predominant infiltrating immune cells mediating that inflammatory process (3). Earlier studies have suggested that proteinuria, renal hypoxia, and/or glomerulus-derived cytokines may induce macrophage recruitment to the kidneys. However, it remains unclear which cell types responds to pathological stimuli and activate inflammatory processes in the kidney, though proximal tubular epithelial cells have been shown to produce the chemokine MCP-1 (3).

Macrophages infiltrating the kidneys produce various proinflammatory cytokines, including TNF-α and IL-1β, as well as metalloproteinases (3). Moreover, the finding that blockade of TNF-α and IL-1β suppresses glomerular inflammation and ameliorates renal damage suggests the infiltrating macrophages contribute in some way to the renal injury (5). Macrophage infiltration also often correlates with the degree of renal fibrosis, and depletion of macrophages reduces fibrosis in several disease models, suggesting that macrophages also contribute to fibrosis (6). On the other hand, macrophages that take up apoptotic cells exhibit antiinflammatory properties and may contribute to resolution of inflammation (7). Indeed, hepatic macrophages were shown to be important for resolution of inflammatory scarring (8). Thus, macrophages likely play multiple, and often opposing, roles in kidney disease and repair (6).

Recent studies demonstrating the diversity of macrophage phenotypes and functionality suggest that the activation state of macrophages may determine their pathogenic or reparative roles in kidney disease (9). In vitro studies have shown that Th1 cytokines, alone or in concert with microbial products, elicit classical M1 activation of macrophages, while Th2 cytokines (IL-4 and IL-13) elicit an alternative form of activation designated M2 (9, 10). M2 macrophages are thought to suppress immune responses and promote tissue remodeling (6, 9, 10), though M2 activation is a rather generic term used to describe various forms of macrophage activation other than classic M1. In addition, the diversity of macrophage activation has been established primarily based on in vitro findings (10), and the phenotypes and functions of M2-type macrophages in vivo are still poorly understood. Very recently it was shown that some, but not all, kidney macrophages exhibit surface expression of Ly-6C (11), which means the macrophage population involved in the renal response to injury is a heterogeneous one. However, the specific functions of the different macrophage subsets are not yet clear.

The renal collecting ducts contribute to the control of water and electrolyte balance. Collecting duct epithelial cells express the water channel aquaporin-2 (AQP2) in their apical plasma membrane and AQP3 and AQP4 in their basolateral membrane (12). Water is transported across the collecting duct epithelium

Conflict of interest: The authors have declared that no conflict of interest exists.
Citation for this article: *J Clin Invest.* 2011;121(9):3425–3441. doi:10.1172/JCI57582.

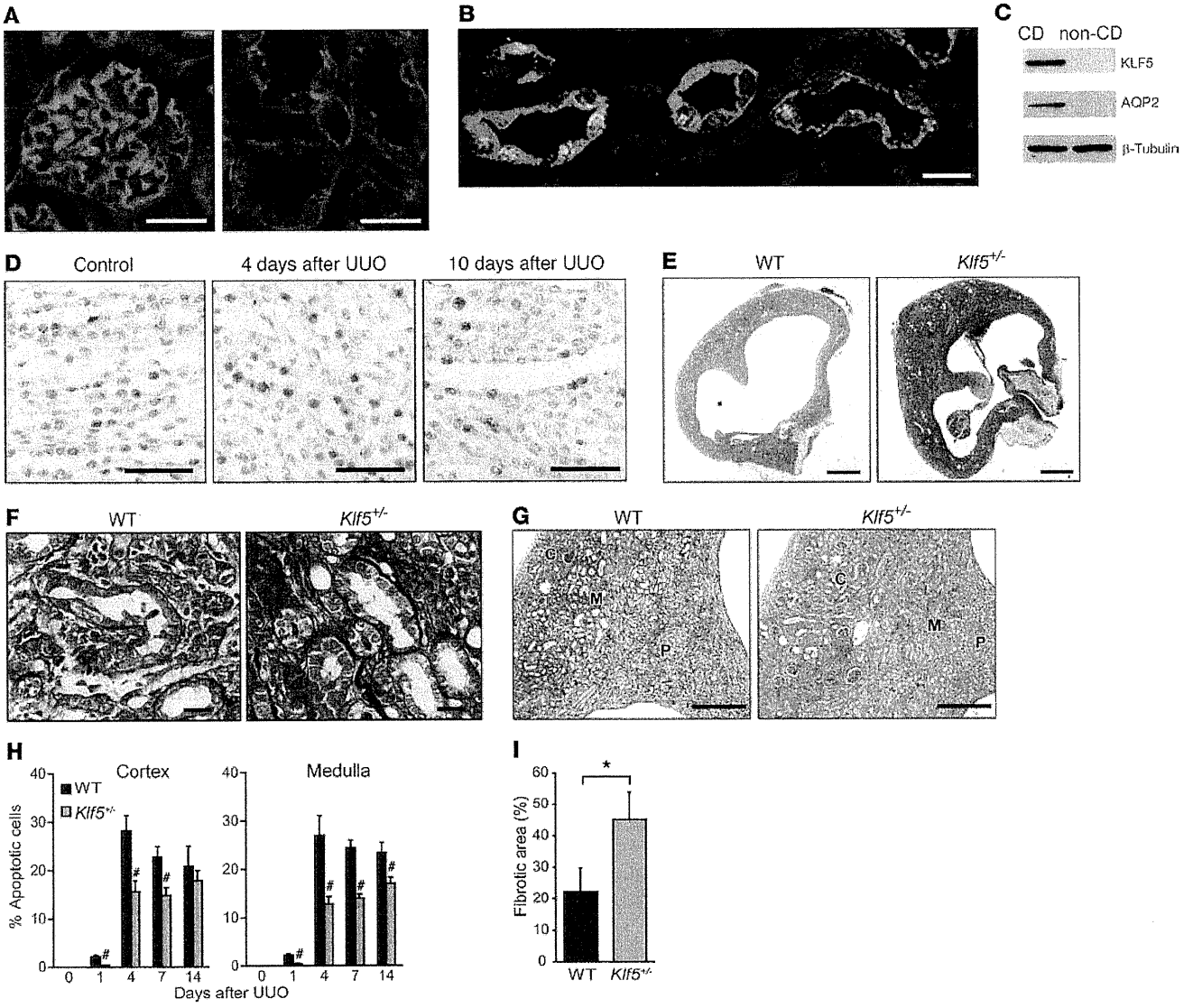

Figure 1

KLF5 is involved in UUO-induced renal injury. (**A**) Immunohistochemical staining of KLF5 (red) in mouse kidneys. Left and right panels show portions of the cortex and medulla, respectively. Nuclei and cell membranes were stained using DAPI (blue) and wheat germ agglutinin (green), respectively. Scale bars: 20 μm. (**B**) KLF5 expression was confined to AQP2-expressing collecting duct cells in papilla. KLF5 (red), AQP2 (green), and nuclei (blue) are shown. Scale bar: 20 μm. (**C**) Expression of KLF5 protein in the collecting duct. Collecting duct (CD) cells were isolated from kidneys by centrifugal separation. The remaining renal cells were non-CD cells. β-Tubulin served as a loading control. (**D**) UUO-induced upregulation of KLF5 in the collecting duct. KLF5 (brown) was detected by immunostaining of sections of medulla under basal conditions (control) and at the indicated times after UUO. Scale bars: 50 μm. (**E**–**G**) Masson's trichrome (**E** and **F**) and H&E (**G**) staining of wild-type and *Klf5*$^{+/-}$ kidneys 14 days after UUO. C, cortex; M, medulla; P, papilla. Scale bars: 1 mm (**E**), 20 μm (**F**), 500 μm (**G**). (**H**) Apoptotic cell fractions in kidneys from wild-type and *Klf5*$^{+/-}$ mice at the indicated days after UUO. Apoptotic cells were analyzed by TUNEL staining, as shown in Supplemental Figure 3A. $^{\#}P < 0.05$ versus wild-type at the same time point. $n = 6$. (**I**) Fibrotic area stained with picrosirius red 14 days after UUO. $^{*}P < 0.05$. $n = 6$. Representative sections are shown in Supplemental Figure 3C.

through those AQPs. AQP2 is abundantly expressed in the connecting tubule (connecting tubule cells), in the cortical and outer medullary collecting ducts (principal cells), and in the inner medullary collecting duct (IMCD cells) and plays an essential role in urinary concentration. Recent studies have shown that collecting duct cells in culture (13, 14) and in the fetal urinary tract obstruction model (15) exhibit a loss in epithelial phenotypes and a concomitant gain in mesenchymal phenotypes through a process often termed "epithelial-mesenchymal transition." This suggests that collecting duct cells are in some way involved in interstitial fibrosis. However, it remains largely unknown whether or how collecting duct cells contribute to tubulointerstitial inflammation.

Members of the Krüppel-like factor (KLF) family of transcription factors are important regulators of development, cellular differentiation, and growth, as well as the pathogenesis of various diseases, including cancer and cardiovascular disease (16). We previously

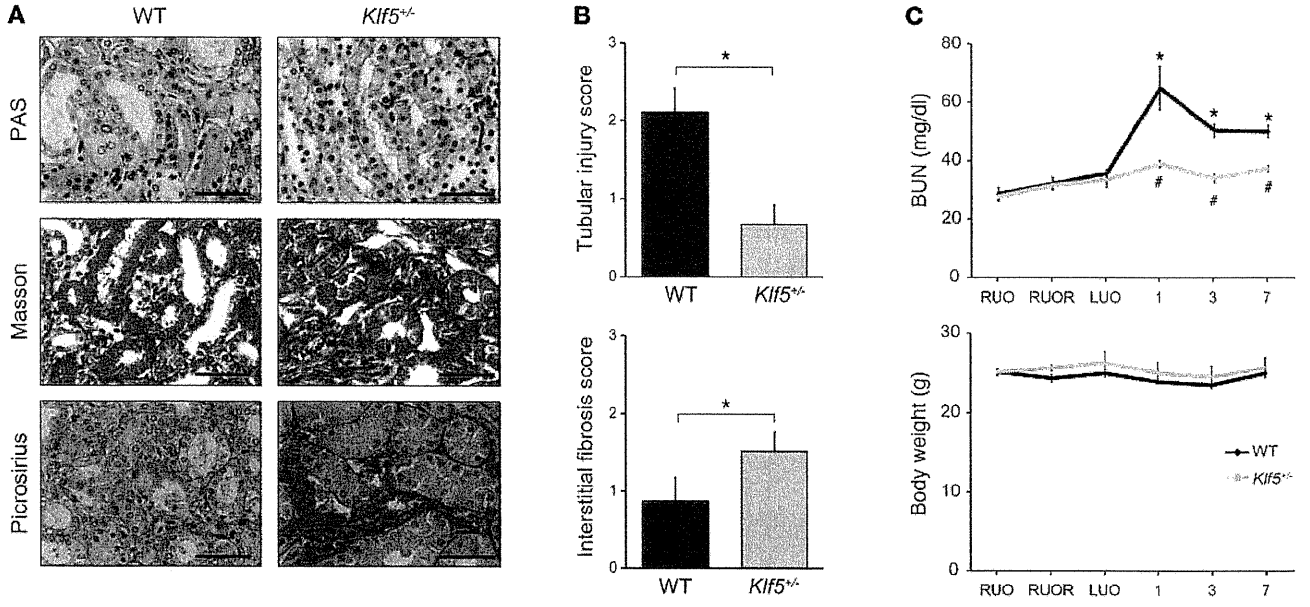

Figure 2

Klf5 haploinsufficiency ameliorated renal dysfunction induced by the reversible UUO. The right ureters of *Klf5*$^{+/-}$ and wild-type mice were transiently obstructed for 3 days; then 7 days after relief of the obstruction, the left ureters were obstructed. (**A**) Representative PAS, Masson's trichrome, and picrosirius red staining of wild-type and *Klf5*$^{+/-}$ right kidneys 7 days after left ureter obstruction. Scale bars: 50 μm. (**B**) Tubular injury and interstitial fibrosis scores are shown. *$P < 0.05$. (**C**) BUN and body weight were measured prior to right ureteral obstruction (RUO), prior to release of the obstruction (RUOR), prior to left ureteral obstruction (LUO), and on indicated days after LUO. $n = 7$ for each group. *$P < 0.05$ versus the baseline of the same genotype. #$P < 0.05$ versus wild-type at the same time point.

showed that KLF5 expressed in cardiac fibroblasts is required for the cardiac hypertrophy and fibrosis that develop in response to continuous infusion of angiotensin II and pressure overload (17, 18). KLF5 also plays a central role in arterial wall remodeling (17, 19). With these results as background, we were interested in whether KLF5 plays a role in renal tubulointerstitial inflammation and fibrosis. We found that *Klf5*$^{+/-}$ mice were protected from renal injury induced by unilateral ureteral obstruction (UUO), but showed enhanced fibrosis. Through a combination of in vitro and in vivo analyses, we further show that collecting duct epithelial cells respond to UUO and initiate the accumulation of M1-type macrophages at least in part through KLF5-dependent production of the secretory proteins S100A8 and S100A9. Our findings demonstrate a previously unappreciated function of collecting duct epithelial cells as central regulators of tubulointerstitial inflammatory processes.

Results

Klf5 is expressed in collecting duct epithelial cells. We first analyzed the distribution of *Klf5* expression in the kidney. Immunohistochemical staining showed that, in normal kidneys, KLF5 is expressed in the nuclei of collecting duct epithelial cells, but not in glomeruli or other tubules (Figure 1A). Consistent with this finding, expression of KLF5 was restricted to cells also expressing AQP2, which is known to be specifically expressed in collecting duct epithelial cells (ref. 20, Figure 1B, and Supplemental Figure 1A; supplemental material available online with this article; doi:10.1172/JCI57582DS1). The collecting duct epithelial cell–specific expression of KLF5 was still further confirmed by its presence in collecting duct cells isolated from kidneys and its absence in non–collecting duct cells (Figure 1C and Supplemental Figure 1B).

Klf5 haploinsufficiency ameliorates renal injury and dysfunction induced by UUO. We next employed the UUO model of tubulointerstitial damage to analyze the role of KLF5 in renal injury (21). We found that UUO increased KLF5 expression in renal collecting duct cells (Figure 1D and Supplemental Figure 1C). Expression of *Klf5* mRNA was readily detected in collecting duct cells, but was barely detectable in CD11b$^+$F4/80$^+$ (monocytes/macrophages), CD31$^+$ (endothelial cells), or α-SMA$^+$ (myofibroblasts, mesangial cells, and smooth muscle cells) cells sorted from kidneys (Supplemental Figure 1C). Upon immunohistochemical staining, KLF5 was detected only in collecting duct cells in sections of normal and day 4 UUO kidneys; a few interstitial cells also stained positive for KLF5 in sections of day 10 UUO kidneys (Figure 1D). These results indicate that high-level *Klf5* expression is largely limited to collecting duct cells.

Under physiological conditions, *Klf5*$^{+/-}$ mice did not exhibit renal dysfunction or pathological changes (Supplemental Figure 2A and Supplemental Table 1). However, when *Klf5*$^{+/-}$ mice were subjected to UUO, they exhibited less renal structural destruction than wild-type mice, as indicated by amelioration of tubular dilation and atrophy, tubular epithelial cell sloughing, and tubular basement membrane thickening (Figure 1, E–G, and Supplemental Figure 2B). Consequently, kidney weight loss and tubular injury score were significantly lower in *Klf5*$^{+/-}$ than wild-type mice (Supplemental Figure 2C). Moreover, significantly fewer apoptotic cells were observed in both the cortex and medulla of kidneys from *Klf5*$^{+/-}$ compared with wild-type mice (Figure 1H and Supplemental Figure 3, A and B). In sharp contrast, interstitial fibrosis was significantly exacerbated in *Klf5*$^{+/-}$ mice, as compared with wild-type mice (Figure

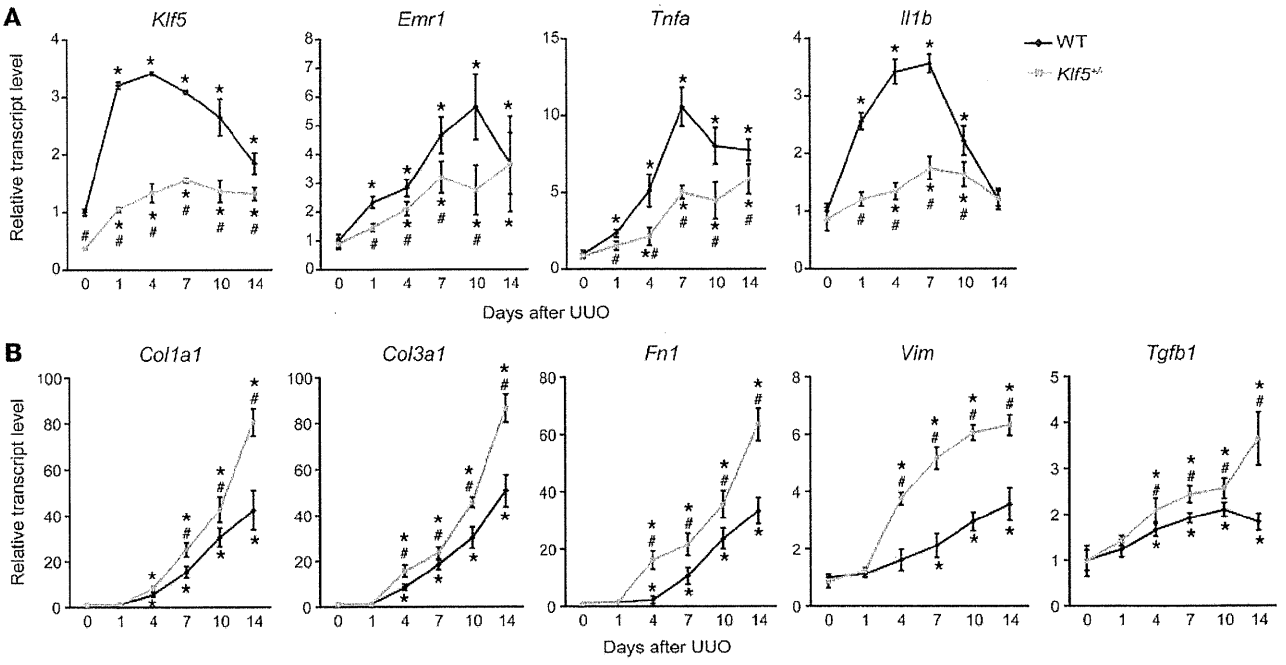

Figure 3
Effects of *Klf5* haploinsufficiency on renal gene expression. Wild-type and *Klf5*$^{+/-}$ mice were subjected to UUO, after which relative transcript levels of genes involved in renal inflammation (**A**) and fibrosis (**B**) were measured at the indicated times using real-time PCR. Data labeled day 0 show gene expression in kidneys under basal conditions. Expression levels were normalized first to those of 18s rRNA and then further normalized to the levels in the kidneys from control wild-type mice. *$P < 0.05$ versus the control (day 0) for the same genotype; #$P < 0.05$ versus wild-type at the same time point. $n = 5$ for each point.

1, E, F, and I, Supplemental Figure 2C, and Supplemental Figure 3, C and D). It thus appears that the *Klf5* haploinsufficiency protected kidneys from the structural destruction induced by UUO, but it promoted fibrosis. Because the contralateral kidneys were uninjured, neither wild-type nor *Klf5*$^{+/-}$ mice showed abnormal blood chemistry, and no mice died within 3 months after UUO (Supplemental Table 2).

To analyze the effects of *Klf5* haploinsufficiency on renal dysfunction, we employed a reversible UUO procedure (22). Initially, the right ureter was obstructed for 3 days, and then the obstruction was released. After mice were allowed to recover for 7 days, the left ureter was ligated to disable contralateral kidney function. After an additional 7 days, the right kidneys of *Klf5*$^{+/-}$ mice exhibited less renal injury than those of wild-type mice (Figure 2, A and B), though fibrosis was more pronounced in the *Klf5*$^{+/-}$ kidney. Blood urea nitrogen (BUN) levels were significantly lower in *Klf5*$^{+/-}$ than wild-type mice, while body weights were not different (Figure 2C). These results demonstrate that *Klf5* haploinsufficiency protected kidneys from dysfunction induced by the transient UUO, despite the apparent augmentation in fibrosis.

Klf5 haploinsufficiency modulates renal inflammation and fibrosis induced by UUO. Recent studies suggest that inflammation is crucially involved in renal cellular injury and fibrosis (23). This prompted us to assess the involvement of KLF5 in inflammatory processes in the kidney. We found that, in wild-type mice, UUO increased renal expression of *Tnfa* and *Il1b*, which encode the proinflammatory cytokines TNF-α and IL-1β, respectively (Figure 3A); that the expression levels were highest 7 days after UUO; and that the levels of these proinflammatory cytokines were significantly reduced in *Klf5*$^{+/-}$ kidneys following UUO. In wild-type kidneys, UUO also increased expression of *Emr1*, which encodes the macrophage marker F4/80, and that effect was significantly reduced in *Klf5*$^{+/-}$ kidneys, suggesting that UUO-induced renal infiltration by macrophages and their inflammatory activation are diminished in *Klf5*$^{+/-}$ kidneys. As expected from the enhanced fibrosis, expression levels of *Col1a1* and *Col3a1*, encoding collagen type I and III, respectively; *Fn1*, encoding fibronectin; *Vim*, encoding vimentin; and *Acta2*, encoding α-SMA, were all significantly increased in *Klf5*$^{+/-}$ kidneys, and their expression was highest 14 days after UUO (Figure 3B). In addition, expression of *Tgfb1*, which encodes the profibrotic cytokine TGF-β1, was also significantly increased in *Klf5*$^{+/-}$ kidneys. As a result, the interstitial area in *Klf5*$^{+/-}$ kidneys was reduced after UUO due to a reduction in the number of apoptotic cells, whereas the fibrotic area and the fibrotic/interstitial area ratio were increased in *Klf5*$^{+/-}$ kidneys (Supplemental Figure 3D). Collectively, these results suggest that *Klf5* haploinsufficiency suppresses early inflammatory processes following UUO, while augmenting fibrotic processes at later times.

Differential recruitment of macrophage subtypes to kidneys after UUO. The reduction in F4/80 expression observed in *Klf5*$^{+/-}$ kidneys suggests that macrophage accumulation was suppressed there. We tested that idea using flow cytometry to assess renal macrophages (Supplemental Figure 4A). In wild-type mice, UUO induced accumulation of CD11b$^+$F4/80$^+$ cells (Figure 4A), and we noted two major subpopulations: CD11b$^+$F4/80^{lo} (R1) and CD11b$^+$F4/80^{hi} (R2). Under basal conditions the CD11b$^+$F4/80^{hi} fraction was significantly larger than the CD11b$^+$F4/80^{lo} fraction (Figure 4B), but the latter was increased from day 1 after UUO, while the former

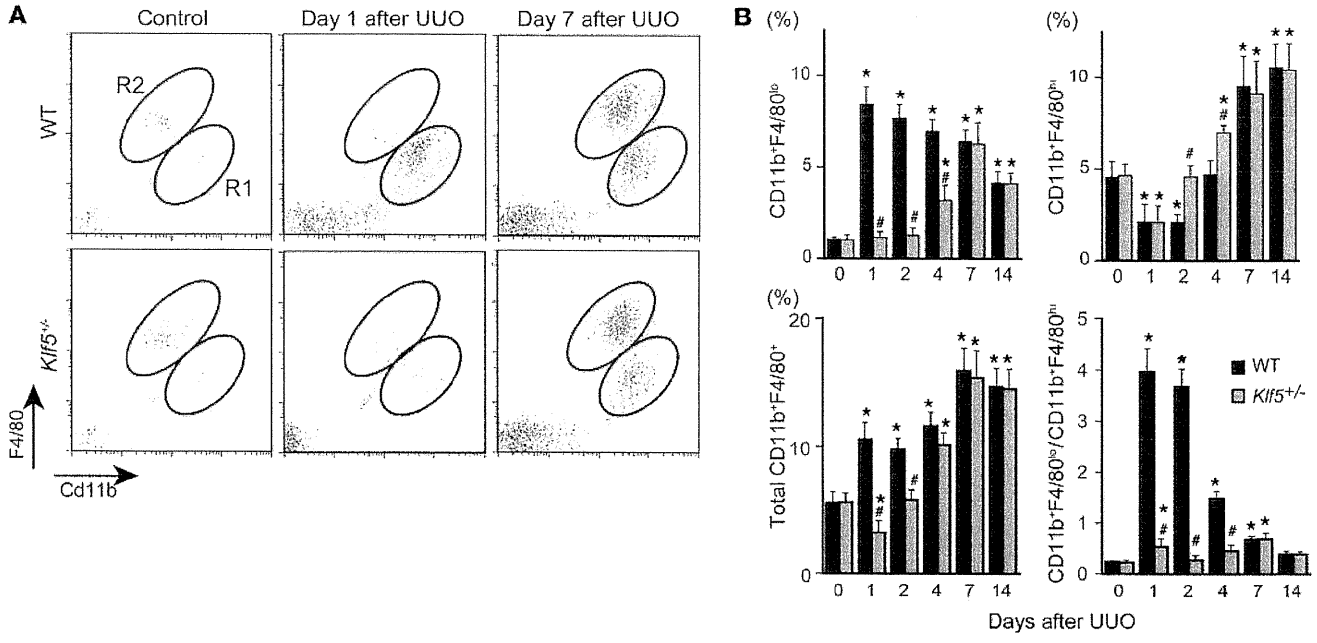

Figure 4

KLF5 controls the recruitment and accumulation of CD11b$^+$F4/80$^+$ cells in response to UUO. (**A**) Representative flow cytometry plots of macrophages in whole kidneys from wild-type and *Klf5*$^{+/-}$ mice subjected to either UUO or sham operation. R1 and R2 indicate CD11b$^+$F4/80^{lo} and CD11b$^+$F4/80^{hi} cells, respectively. (**B**) Fractions of CD11b$^+$F4/80^{lo} (region R1 in **A**), CD11b$^+$F4/80^{hi} (R2), and total CD11b$^+$F4/80$^+$ cells among total live cells and the ratios of CD11b$^+$F4/80^{lo} to CD11b$^+$F4/80^{hi} cells isolated from the kidneys of wild-type and *Klf5*$^{+/-}$ mice subjected to UUO. $^*P < 0.05$ versus day 0 of the same genotype; $^\#P < 0.05$ versus wild-type at the same time point. $n = 6$ for each group. The cell populations expressed as fractions of total macrophages and numbers of cells per kidney are shown in Supplemental Figure 5, A and B.

was reduced on days 1 and 2. As a result, the ratio of CD11b$^+$F4/80^{lo} to CD11b$^+$F4/80^{hi} cells was significantly increased from day 1 to day 7. The cell ratio then declined to the basal level within 14 days after UUO.

We next characterized the surface phenotypes of CD11b$^+$F4/80$^+$ cells and found that while CD11b$^+$F4/80^{lo} cells were Ly-6C$^+$, CD11b$^+$F4/80^{hi} cells were Ly-6C$^{-/lo}$, and majorities of both cell populations were negative for the granulocyte marker Ly-6G (Supplemental Figure 4B). They were also negative for the myeloid-derived suppressor cell marker CD93 (24). In addition, while both CD11b$^+$F4/80^{lo} and CD11b$^+$F4/80^{hi} cells showed greater forward scatter (FSC) on day 7 than day 1 after UUO, CD11b$^+$F4/80^{hi} cells showed much greater FSC than CD11b$^+$F4/80^{hi} cells on day 7 (Supplemental Figure 4C). In Cytospin preparations, CD11b$^+$F4/80^{lo} cells exhibited a small, monocytoid morphology on day 1 but also included larger cells by day 7 (Supplemental Figure 4D). In contrast, CD11b$^+$F4/80^{hi} cells were larger than CD11b$^+$F4/80^{lo} cells and had a fried egg–like morphology. Despite their monocytoid morphology, day-1 CD11b$^+$F4/80^{lo} cells showed higher surface F4/80 and CD11b levels than circulating CD11b$^+$Ly-6C$^+$ inflammatory monocytes, which have been shown to be recruited to kidneys after UUO (11). This suggests CD11b$^+$F4/80^{lo} cells include macrophages as well as monocytes that had been recruited to the kidneys, where they are undergoing differentiation into macrophages (11, 25), while CD11b$^+$F4/80^{hi} cells are more mature macrophages. Moreover, CD11b$^+$F4/80^{hi} cells but not CD11b$^+$F4/80^{lo} cells were positive for CD206 and CD301, markers of M2-type activation. Collectively then, the two populations of CD11b$^+$F4/80$^+$ cells in UUO kidneys exhibited a CD11b$^+$F4/80^{lo}Ly-6C$^+$CD206$^-$CD301$^-$ phenotype, which is indicative of M1-type activation, and a CD11b$^+$F4/80^{hi}Ly-6C$^{-/lo}$Ly-6G$^-$CD206$^+$CD301$^+$ phenotype, which is indicative of M2-type activation (11, 26).

Under basal conditions there were no significant differences in the CD11b$^+$F4/80^{lo} and CD11b$^+$F4/80^{hi} fractions between wild-type and *Klf5*$^{+/-}$ kidneys (Figure 4B and Supplemental Figure 5, A and B). However, *Klf5*$^{+/-}$ kidneys contained significantly fewer CD11b$^+$F4/80^{lo} cells from day 1 to day 4 after UUO. By contrast, *Klf5*$^{+/-}$ kidneys contained more CD11b$^+$F4/80^{hi} cells on days 2 and 4 than wild-type kidneys (Figure 4B and Supplemental Figure 5, A and B). As a result, the CD11b$^+$F4/80^{lo} to CD11b$^+$F4/80^{hi} ratio was significantly higher than baseline only on days 1 and 7 in *Klf5*$^{+/-}$ kidneys. Reduced inflammatory monocyte/macrophage infiltration into *Klf5*$^{+/-}$ kidneys 1 day after UUO was further confirmed by immunohistochemical staining for F4/80 and Ly-6C (Supplemental Figure 5, C and D). Taken together, these findings suggest that CD11b$^+$F4/80^{lo} and CD111b$^+$F4/80^{hi} cells differentially accumulate in the kidney during the course of the response to UUO. At early times, when apoptosis and tissue destruction are occurring, primarily CD11b$^+$F4/80^{lo} monocytes/macrophages accumulate in kidneys. Later, when tissue remodeling and fibrosis dominate, the numbers of CD11b$^+$F4/80^{hi} macrophages are increased. *Klf5* haploinsufficiency reduces accumulation of CD11b$^+$F4/80^{lo} cells and increases CD11b$^+$F4/80^{hi} cells at earlier time points, thereby altering the balance of macrophage polarity during the response to UUO.

Renal CD11b$^+$F4/80$^+$ cells are phenotypically different from splenic classical DCs. DCs have been identified in kidneys (27–29). Although CD11c has been used to distinguish renal DCs from macrophages (30), the marker is widely expressed and is induc-

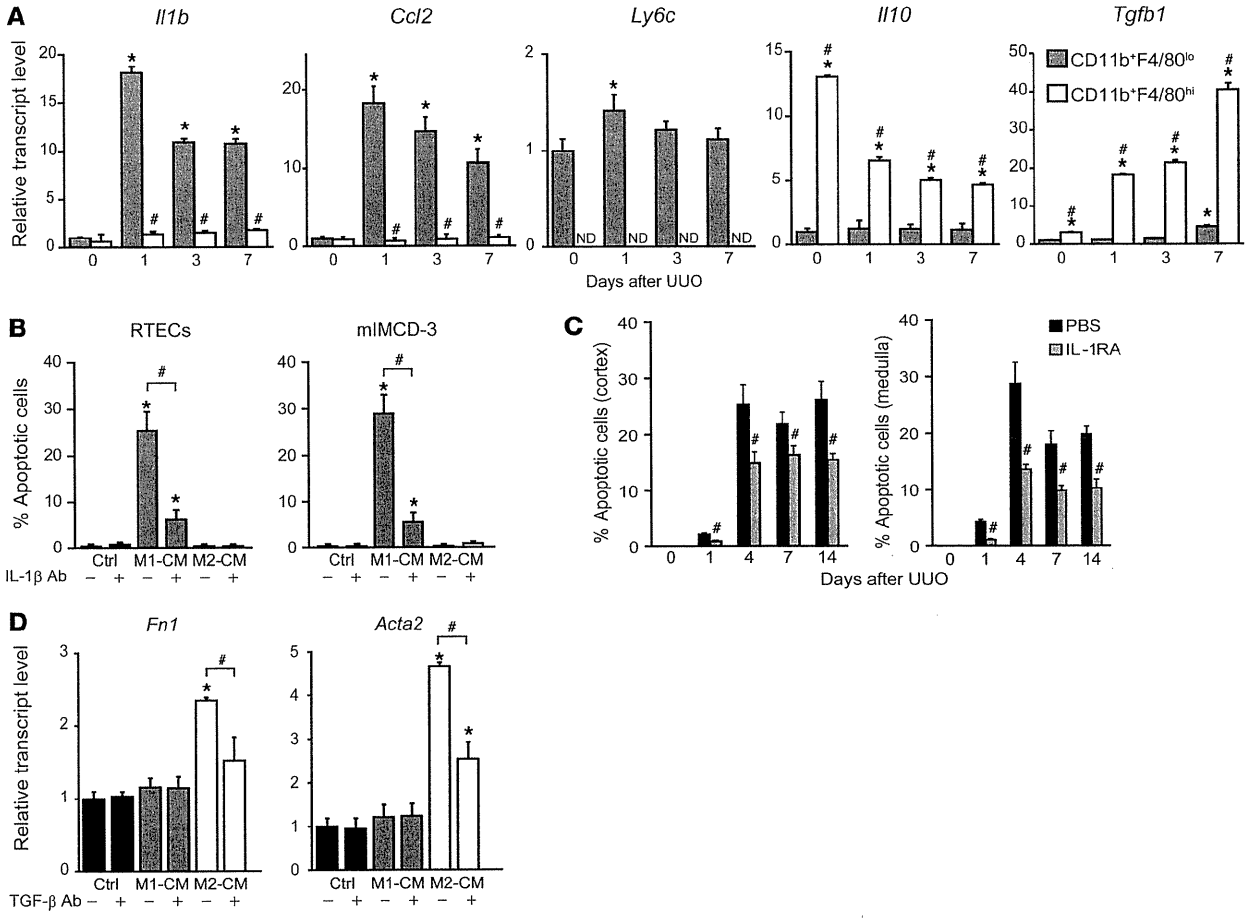

Figure 5

Differential involvement of CD11b$^+$F4/80^{lo} and CD11b$^+$F4/80^{hi} cells in renal responses to UUO. (**A**) mRNA expression in CD11b$^+$F4/80^{lo} and CD11b$^+$F4/80^{hi} cells isolated from kidneys under basal conditions (day 0) or after UUO. Expression levels were normalized to those of 18s rRNA and then further normalized to the levels in the resident CD11b$^+$F4/80^{lo} cells isolated from normal kidneys of wild-type mice. $n = 3$. $^{\#}P < 0.05$ versus CD11b$^+$F4/80^{lo} cells from wild-type mice at the same time point. $^*P < 0.05$ versus day 0 of the same population. ND, nondetectable. (**B**) Effects of conditioned medium (CM) prepared by incubating CD11b$^+$F4/80^{lo} or CD11b$^+$F4/80^{hi} cells isolated from kidneys 1 (CD11b$^+$F4/80^{lo}) or 7 (CD11b$^+$F4/80^{hi}) days after UUO in serum-free RPMI medium for 24 hours. Serum-free RPMI containing 0.3% BSA was used as a control medium (Ctrl). Fractions of TUNEL$^+$ apoptotic primary mouse RTECs and mIMCD-3 cells after culture in the CM with either control IgG or IL-1β neutralizing antibody for 24 hours. $n = 6$. Expression levels were normalized to those of 18s rRNA and then further normalized to the levels in cells treated with the control medium. $^*P < 0.05$. versus cells in control medium with control IgG; $^{\#}P < 0.05$. (**C**) Effects of IL-1RA administration on UUO responses. Renal phenotypes of wild-type mice intraperitoneally administered either PBS (vehicle) or IL-1RA (200 μg daily). $^{\#}P < 0.05$ versus the PBS group at the same time point. $n = 6$. (**D**) Levels of *Fn1* and *Acta2* transcription in 10T1/2 embryo fibroblasts cultured for 24 hours in CM as in **B** with either control IgG or TGF-β neutralizing antibody. $^*P < 0.05$ versus cells in control medium with control IgG; $^{\#}P < 0.05$. $n = 3$.

ible in macrophages and other immune cells during inflammation (31). To better characterize renal CD11b$^+$ cells in comparison with bona fide DCs, we assessed the expression of multiple DC markers in renal CD11b$^+$ cells and splenic classical DCs (Supplemental Figure 6). We found that CD11b$^+$F4/80^{lo} cells were CD11c^{lo}MHCII$^{-/+}$CD86$^-$CD83$^-$, which supports the notion that they are monocytes/macrophages. CD11b$^+$F4/80^{hi} cells were CD11c^{int}MHCII$^+$CD86$^+$CD83$^-$. As compared with splenic classical DCs, CD11c levels were lower in renal CD11b$^+$F4/80^{hi} cells, and CD83, a marker for mature DCs (32, 33), was not expressed. In Cytospin preparations, CD11b$^+$F4/80^{hi} cells contained vacuolar cytoplasm and lacked cytoplasmic extensions, which are macrophage-like characteristics and different from those of splenic DCs (Supplemental Figure 4D and Supplemental Figure 7A). These results indicate that renal CD11b$^+$F4/80^{hi} cells express several DC markers, but their phenotypes differ from those of splenic classical DCs.

Because we were not able to identify a cell population that resembled splenic DCs among the CD11b$^+$ cells, we tested whether cells expressing high levels of CD11c might be present among the renal leukocytes (CD45$^+$ cells). We found that CD11c^{hi} cells were present and were CD11c^{hi}MHCII$^+$CD86$^+$CD83$^+$CD11b$^-$F4/80^{lo}, which is a phenotype that closely resembles that of splenic DCs (Supplemental Figure 6D). In Cytospin preparations, moreover, renal CD11c^{hi} cells had pleomorphic nuclei and cytoplasmic extensions, and were morphologically similar to splenic DCs (Supplemental Figure 7B). The renal CD11c^{hi}MHCII$^+$CD83$^+$ cells were widely distributed on FSC/side scatter (SSC) plots, and the majority was found

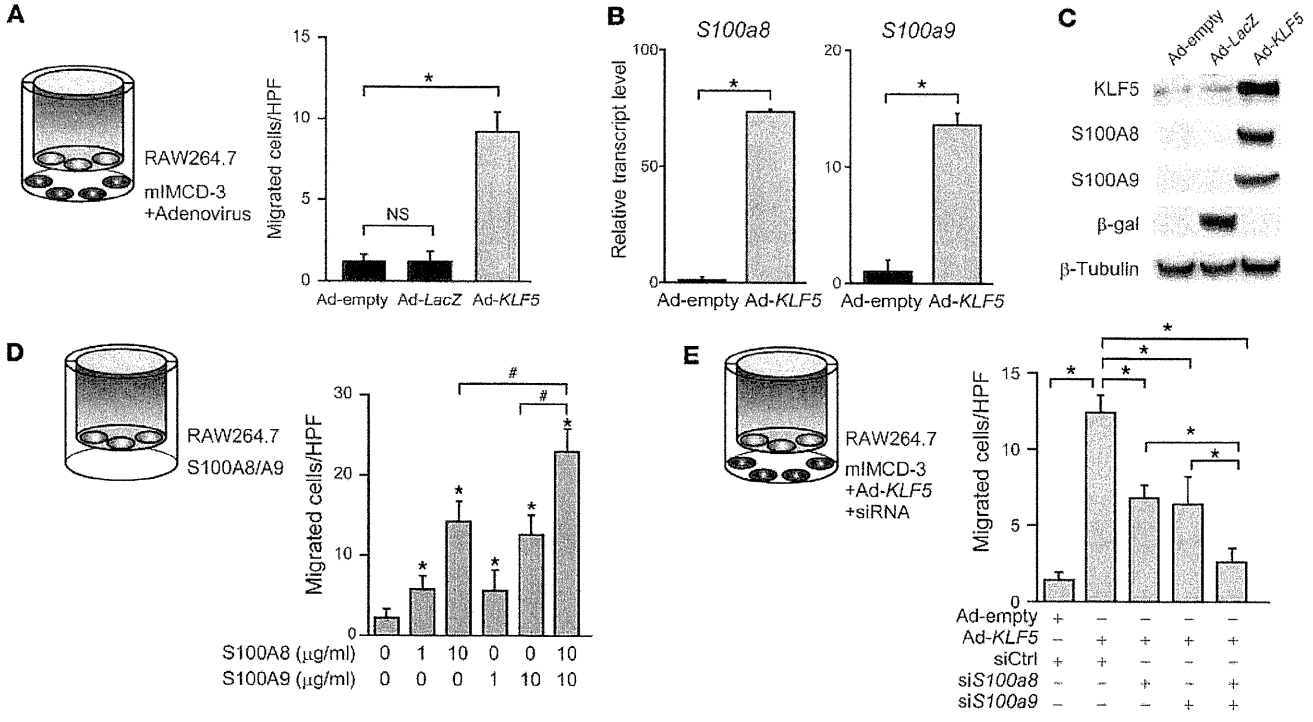

Figure 6

KLF5 induces accumulation of M1 macrophages via S100A8 and S100A9. (**A**) Activation of RAW264.7 macrophage migration by mIMCD-3 cells overexpressing KLF5. As shown schematically, mIMCD-3 and RAW264.7 cells were plated in the bottom wells and inserts, respectively. The mIMCD-3 cells were infected with empty adenovirus (Ad-empty), adenovirus expressing β-galactosidase (Ad-*LacZ*), or adenovirus expressing KLF5 (Ad-*KLF5*), as indicated. The numbers of cells that migrated through the porous membranes per high-power field (HPF) during the 8-hour incubation are shown. $n = 12$. $^*P < 0.05$. (**B** and **C**) Levels of *S100a8* and *S100a9* transcription in mIMCD-3 cells overexpressing KLF5. Relative levels of *S100a8* and *S100a9* transcripts were determined by real-time PCR (**B**). $n = 6$. $^*P < 0.05$. In **C**, expression of KLF5, S100A8, S100A9 protein and β-galactosidase were assessed by Western blotting. β-Tubulin was used as a loading control. (**D**) Effects of recombinant S100A8 and S100A9 on RAW264.7 cell migration. Recombinant S100A8 and/or S100A9 were added to the medium in the lower wells, as shown. $n = 6$. $^*P < 0.05$ versus migrated cells without S100 proteins; $^\#P < 0.05$. (**E**) Effects of *S100a8* and/or *S100a9* knockdown in mIMCD-3 cells overexpressing KLF5 on RAW264.7 migration. mIMCD-3 cells overexpressing KLF5 were transfected with siRNAs against *S100a8* and *S100a9* or control siRNA (siCtrl), as indicated, after which they were plated in the bottom wells, as shown. The numbers of RAW264.7 cells that migrated during the 8-hour incubation are shown. $n = 6$. $^*P < 0.05$.

outside of the R3 gate that was used to characterize CD11b$^+$ cells (Supplemental Figures 4A and 7C), indicating that these cells were not included in our CD11b$^+$F4/80^{hi} and CD11b$^+$F4/80^{lo} cell populations. In addition, the renal CD11c^{hi}MHCII$^+$CD83$^+$ cell fractions were not affected by UUO or *Klf5* haploinsufficiency, making it unlikely that these cells contribute to the renal phenotypes observed in *Klf5*$^{+/-}$ mice (Supplemental Figure 7D). Collectively then, it appears that kidneys contain a CD11c^{hi}MHCII$^+$CD83$^+$ cell population that closely resembles classical DCs. By contrast, the surface marker profile and cellular morphology of CD11b$^+$F4/80^{hi} cells are different from those of classical DCs. Because they differ from both splenic classical DCs and renal classical DC-like cells, and more resemble tissue macrophages in other tissues (34), we will refer to CD11b$^+$F4/80^{hi} cells as macrophages hereafter.

CD11b$^+$F4/80^{lo} and CD11b$^+$F4/80^{hi} cells differentially affect epithelial and mesenchymal cells. To analyze the functions of renal CD11b$^+$F4/80$^+$ cells in more detail, we isolated them from kidneys at various times after UUO (Supplemental Figure 8A). Analysis of mRNA expression in CD11b$^+$F4/80^{lo} and CD11b$^+$F4/80^{hi} cells isolated 0, 1, 3, and 7 days after UUO showed that levels of *Il1b* and *Ccl2* transcripts, encoding the proinflammatory cytokines IL-1β and MCP-1, respectively, were much higher in CD11b$^+$F4/80^{lo} than CD11b$^+$F4/80^{hi} cells (Figure 5A), suggesting that CD11b$^+$F4/80^{lo} cells promote inflammation. *Ly6c* was expressed in CD11b$^+$F4/80^{lo} cells, but was undetectable in CD11b$^+$F4/80^{hi} cells. By contrast, CD11b$^+$F4/80^{hi} cells showed higher levels of *Il10* and *Tgfb1* transcripts, encoding the antiinflammatory cytokines IL-10 and TGF-β1, respectively, which suggests the CD11b$^+$F4/80^{hi} M2-type macrophages are involved in fibrosis and resolution of inflammation. However, CD11b$^+$F4/80^{hi} cells did not express two other M2 markers, *Ym1* and *Fizz1* (data not shown), indicating that the characteristics of CD11b$^+$F4/80^{hi} cells do not perfectly match those of the M2 macrophages previously studied in vitro (9).

To further investigate the functional differences between CD11b$^+$F4/80^{lo} and CD11b$^+$F4/80^{hi} cells, we incubated cultured primary mouse renal tubular epithelial cells (RTECs) and mIMCD-3 mouse collecting duct epithelial cells in medium conditioned by either CD11b$^+$F4/80^{lo} or CD11b$^+$F4/80^{hi} cells isolated from kidneys subjected to UUO. The surface phenotypes and cytokine gene expression profiles of CD11b$^+$F4/80^{lo} and CD11b$^+$F4/80^{hi} cells cultured for 24 hours were similar to those of the cells just after